Technische Universität München
Lehrstuhl für Kommunikationsnetze
Prof. Dr.-Ing. Wolfgang Kellerer

Bachelor's Thesis

Network Planning for the Future Railway Communications

Author:	Lin Huang, Peng
Address:	Clemensstr. 118
	80796 München
	Germany
Matriculation Number:	03764265
Supervisors at TUM:	PD Dr.-Ing. habil. Carmen Mas Machuca
	M.Sc. Cristian Bermudez Serna
Supervisor at UPC:	Dr. José Antonio Lázaro Villa
Begin:	01. April 2022
End:	26. July 2022

With my signature below, I assert that the work in this thesis has been composed by myself independently and no source materials or aids other than those mentioned in the thesis have been used.

München, 26.07.2022
-----------------------------   ------------------------------
Place, Date   Signature

München, 26.07.2022
-----------------------------   ------------------------------
Place, Date   Signature

Abstract

Smart Transportation Systems are changing the way we conceive the future of mobility. In particular, railways are undergoing a transformation process to modernize public transportation and rail operation. Technologies like 5G, optical fiber and the cloud have emerged as catalysts to digitalize the railway by providing high-speed and low-latency communications.

This bachelor's thesis focuses on the exploration of networks enabling train control and on-board data communications. The goal is to plan the network infrastructure (dimensioning and resource allocation) needed for the future communications in the train mobility scenario for Deutsche Bahn's long-distance railway system in Germany.

In this work, we propose a network architecture that can meet the performance requirements of train and passenger applications. We present an approach for 5G base station placement along the rail tracks to guarantee the necessary throughput at the cell edge. Finally, we introduce the data center placement and assignment problem. The objective is to find the required number of data centers and their location in the network, and to assign them to each train station. We perform simulations in four different scenarios, in which we modify input parameters such as the maximum tolerated latency and the maximum number of data centers. The obtained results show the trade-off between the achieved latency and the infrastructure cost.

Contents

Chapter 1

Introduction

Designing the mobility of the future means keeping up with the pace of change today. The high volume of commuters and their need for even greater speed and connectivity presents a growing challenge for railway network operators. Furthermore, it is expected that the need for on-board communications for train control operations will increase with the development of Smart Rail Systems. Existing infrastructures are reaching their limits and need to be expanded while ensuring the smooth operation of existing networks.

In December 2019, the European Commission presented the European Green Deal – a roadmap for making the economy of the European Union (EU) more sustainable. The objective is to accelerate emissions reduction and make Europe climate-neutral by 2050 [1]. Rail transportation systems are recognized as an alternative green means of transport for goods and people because of their larger carrying capacity, energy efficiency, and significantly lower environmental impact compared to conventional transportation systems.

In parallel, the Commission also intends to implement new measures to better adapt the EU single market to the digital era and achieve technological sovereignty [2]. In this sense, emerging technologies like 5G, optical fiber and the cloud have a significant transformative potential in the design of the mobility of the future. These technologies will be a catalyst for the digitalization of the railway and can help the EU achieve its goal of climate neutrality and implement its digital strategy.

Objective and Outline of the Thesis

This bachelor's thesis is part of the AI-NET ANTILLAS (Automated Network Telecom Infrastructure with inteLLigent Autonomous Systems) project. The scope of this project is to develop infrastructure elements for automatized telecommunications networks, which can support the requirements of future applications such as Smart Manufacturing, Smart Transportation Systems and others. The Technical University of Munich (TUM) contributes to ANTILLAS with the subproject SOLA (reSOurce aLlocAtion) focusing on the development of mechanisms for efficient reconfigurable networks.

As an initiative in ANTILLAS-SOLA, it is planned to continue with the exploration of the Smart Transportation Systems scenarios, as it was done for Space-Air-Ground networks by Amir Varasteh et al. in [3] and [4]. This bachelor's thesis focuses on the exploration of networks enabling train control and on-board data communications. It aims to plan the network infrastructure (dimensioning and resource allocation) necessary for the future communications in the train mobility scenario. Here, special

attention will be given to the planning of the access network composed of base stations and data centers and their interconnection to the core network for the Deutsche Bahn's long-distance railway system in Germany.

The proposed network will enable future applications such as Automatic Train Operation (ATO), leveraging of cloud technologies, and meeting bandwidth requirements of data-hungry passengers. Nowadays, low bandwidth networks such as GSM-R, providing less than 200 kbps of peak data rate [5], are being used to transmit train control information. Moreover, even though trains may use multiple on-board technologies such as repeaters and access points to provide users with an internet connection, they fail in their attempts since these connections are characterized by having low throughputs (less than 2 Mbps) and constant service interruptions.

The main goal of this thesis is to find solutions to the following questions:

1. Which network technologies may be enablers for the digital transformation of the railway?
2. Where to place network components such as base stations and data centers?
3. How to interconnect the network components (network topology)?

Given:

1. Train mobility patterns and traffic profiles.
2. Service requirements in terms of bandwidth, delay, reliability level, and availability.

The results from this bachelor's thesis can be useful to get an insight into requirements for Smart Transportation Systems, which may in turn be helpful to lay the foundations for other scenarios such as Autonomous Driving and Tele-Operated Driving.

Thesis Structure

The thesis is structured as follows: In Chapter 2, all background necessary to understand the thesis is introduced, including the proposed network architecture for the rail environment. In Chapter 3, we describe the deployment scenario, model the network with a graph, and present an approach to solve the Base Station Placement Problem (BSPP). Furthermore, in Chapter 4, we use an integer linear programming formulation to solve the Data Center Placement and Assignment Problem (DCPAP), explain the different scenarios considered in the simulations, and interpret the results. Finally, Chapter 5 concludes the thesis with the conclusions and ideas for future work.

Chapter 2

Background

2.1 Rail Communication Systems

In train mobility scenarios, 2 types of communication services can be distinguished:

- Digital Rail Operations, which include communication services necessary for train movement and rail management.

- Passenger connectivity (Gigabit Train), which offers reliable and high-performance connectivity for passengers on the train.

2.1.1 Digital Rail Operations

Digital Rail Operations (DRO) involve all communication services and mobile applications needed for running trains as well as those required to improve railway management. These applications can be split into two categories as defined in [6]:

- Critical communication applications, that are necessary for the safety and movement of trains, or required by law, e.g., emergency communications and Automatic Train Operation (ATO).
- Performance communication applications, that are used to optimize the performance of railway operation, e.g., train departure and telemetry.

The Control Command and Signaling Technical Specification for Interoperability (CCS TSI) is the EU's legal framework for railways. It specifies GSM-R as the radio standard to be used for communication between trains and railway regulation control centers [7]. GSM-R is implemented across the world, including all EU member states and countries in Asia and northern Africa. However, suppliers have warned their clients about the obsolescence of GSM-R technology between 2025 and 2035, advising them to prepare for replacement [8].

Currently, the International Union of Railways (UIC) and other international organisms are working on standardizing the Future Railway Mobile Communication System (FRMCS), the successor of GSM-R, based on 5G technology. It is expected to provide a low-latency and spectrally efficient foundation, which will be essential for critical applications as they are part of the Ultra-Reliable Low Latency Communication (URLLC) 5G use case. However, FRMCS will also include some performance applications [9].

Dedicated and harmonized frequency bands are expected to be available for FRMCS deployments, especially for critical applications. The Electronic Communications Committee approved the official decision to allocate 2 x 5.6 MHz in the 900 MHz band with Frequency Division Multiplexing (FDD) and 10 MHz in the 1900 MHz band with Time Division Duplexing (TDD) for European railways under harmonized conditions in November of 2020 [10].

The main applications of DRO can be split into the following use cases:

- Voice and data services for staff and infrastructure: Passenger surveillance, railway emergency calls, and telemetry applications are some examples.

- ETCS: The European Train Control System is a train-protection system based on radio signals. Track-to-train communication is necessary to provide the train position and speed to the trackside Radio Block Center, from which the trains will get movement authorizations.

- ATO: Automatic Train Operation will allow improved train control in terms of train acceleration and deceleration, for instance, to improve train schedules and energy efficiency.

- Critical video: For increased degrees of railway automation, critical video transmission, which includes the transmission of important lidar and radar sensor data, is likely to become necessary. Remote access to camera and sensor data from trains will also be required for driverless railway operation.

Table 1 shows the estimated requirements for the main applications of DRO.

Use case	Message type	UL/DL	Data rate	Latency	Packet reliability
Voice	Audio	50/50	24 kbps	100 ms	99.9%
ETCS	Position report	UL	10 kbps	100 ms	99.9999%
	Movement authority	DL	10 kbps	100 ms	99.9999%
ATO	Journey profile	DL	10-50 kbps	100 ms	99.9%
	Segment profile	DL	100 kbps	1 s	99.9%
	Status report	UL	1 kbps	100 ms	99.9%
Remote driving	Video/Audio stream	UL	1-7 Mbps	10 ms	99.9%
	Control data	DL	10-100 kbps	10 ms	99.9999%
Video surveillance	Video/Audio stream	UL	1-7 Mbps	100 ms	99.9%

Table 1 Requirements for selected Digital Rail Operations applications [11]

2.1.2 Passenger Connectivity

Passengers are increasingly demanding stable and high-performance connectivity, which influences their choice of mode of transportation. As a result, connectivity has emerged as a strong socio-economic driver. Modern high-speed trains like the German InterCity Express (ICE) can be compared to small and digitally active villages of up to 1,000 people, traveling through the country at speeds of up to 300 km/h.

The goal of the Gigabit Train concept is to provide passengers on board high-speed trains with the same level of connectivity as the one they would have at home or work. The growing number of rail passengers, along with their increased use of digital applications, drives up demand for mobile connectivity on trains. Projections until 2030 for a train carrying up to 1,000 passengers predict a demand of 200 Mbps by 2020, 800 Mbps by 2028, and a minimum of 1 Gbps by 2030 [8].

This level of connectivity demands innovations in two main areas: trackside coverage and on-board connectivity hardware. Providing cellular trackside coverage will be a challenge for Mobile Network Operators (MNOs) due to the high speed of trains and the effect it has on the transmitted signals, e.g., the Doppler effect. However, transferring the trackside signal into the train is another problem to be considered as considerable penetration loss is expected from the train's metal body.

There are two models of connectivity inside a train as shown in Figure 1:

- Direct connectivity: Passengers use their own subscription and connect directly to their MNO. To make this possible, the MNO's licensed spectrum has to be available inside the train using a repeater to extend the signal inside the train. The repeater is needed to compensate for the penetration losses caused by the metalized windows and train carriage on the radio signal.

- Indirect connectivity: Railway Operators provide Internet access to their passengers via Wi-Fi and Voice is provided via Voice over Wi-Fi. Antennas are installed on the roof of trains and the data signal is transported to multiple Access Points (APs) along the train to provide complete coverage.
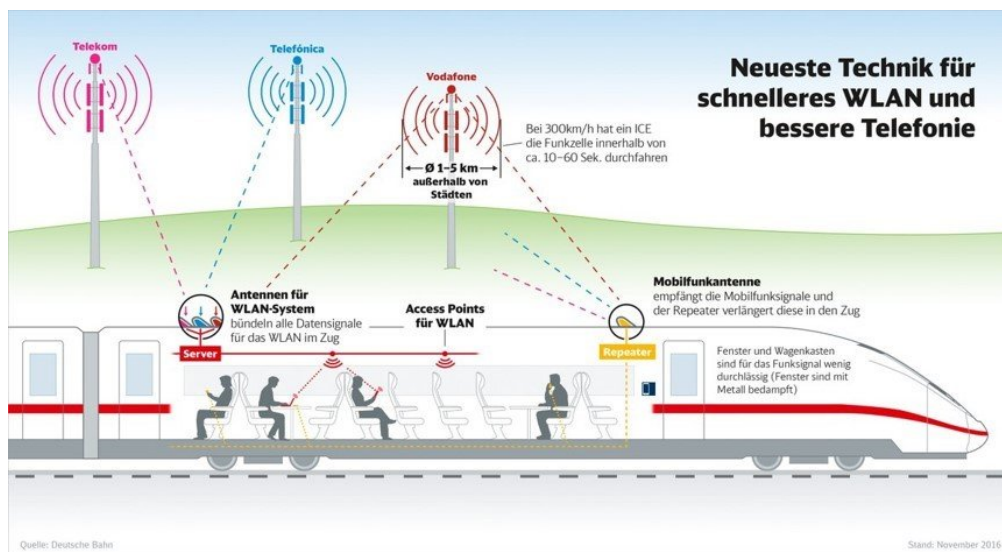

Figure 1 Direct and indirect connectivity inside a train [12]

Passenger connectivity on trains is part of the Enhanced Mobile Broadband (eMBB) 5G use case. The estimated performance requirements for the main communication services for passengers in the rail environment are summarized in Table 2.

Key Performance Indicator (KPI)	Passenger service (eMBB) requirement
Latency (min. between user service end-points)	Non-Critical
User data rate (max.)	~10 Mbps/passenger
Reliability (%)	Not Critical
Availability (%)	Not Critical
Traffic Density (Traffic demand per specific area)	Max. 1-2 Gbps. Assuming 5-10 Mbps/passenger @ train or station. Total: 100-300 passengers in a cell coverage area, ~max. avg. 1-2 Gbps
Device Density (#Devices per specific area)	100-300 passengers per cell coverage area

Table 2 Requirements foreseen in 5G landscape for passenger connectivity [13]

2.2 Cooperation Models

As already mentioned in the previous section, there are two kinds of customers on board trains: the rail passenger using on-board public Wi-Fi and the MNO customer with an Internet data plan. These two types of customers are served by two different service providers: the Infrastructure Manager (IM), like DB Netz AG, and the Mobile Network Operator (MNO), such as Vodafone. Both must rely on the same public mobile network, since it is the only infrastructure available that is capable of meeting connection demands.

Mobile communications for the rail environment require building a special-purpose rail-dedicated active (e.g., 5G equipment for network slicing) and passive (e.g., antenna masts along the tracks and optical fiber cables) network. This deployment is more expensive than current mobile network designs targeting area coverage. Typically, the passive infrastructure accounts for 70-80% of the total cost [8].

For this reason, it is expected that cooperation models between MNOs and IMs need to be developed in order to overcome the low economic viability of infrastructure deployment. It is crucial to leverage sharing of passive infrastructures, such as base stations, power supply installations and optic fiber transmission systems, to increase cost efficiency and potentially allow the use of rail-owned infrastructure. Nevertheless, it should be noted that the utilization of public networks for rail operation is subject to national regulatory, liability and legal constraints.

2.3   Network Architecture for Rail

In this section, a 5G network architecture is proposed for the rail environment (5G-R) based upon an exhaustive review of the state of the art.

2.3.1 Access Network

A) Cloud-Based Dual-Band Hybrid 5G-R Wireless Network

Starting with the Radio Access Network (RAN), the authors of [14] defend the advantages of hybrid networking using both low (sub-6GHz) and high (mmWave) frequency bands to meet the different performance requirements of train-related and passenger-oriented services. To guarantee the mobility performance of the entire network, a cloud-based control/user plane (C/U-plane) decoupled network architecture is proposed in [15].

On the one hand, DRO services can be allocated to sub-6GHz Remote Radio Units (RRUs) without C/U-plane decoupling to get omnidirectional and robust coverage. On the other hand, high-data-rate services, such as passenger connectivity, can benefit from C/U-plane decoupling. The C-plane signaling is carried by sub-6GHz RRUs to achieve reliable transmission, and the U-plane is moved to mmWave RRUs to gain high transmission capacity.
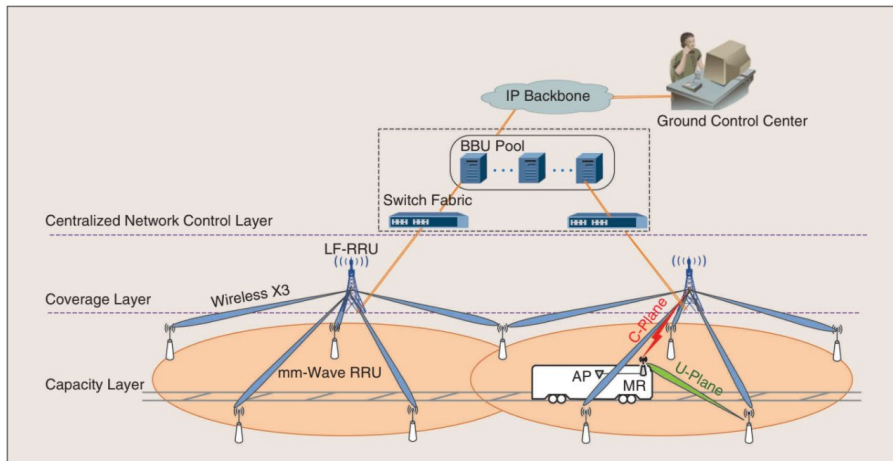
Figure 2 Proposed RAN architecture [15]

In order to improve the utilization of trackside baseband resources, the whole network is based on the Cloud Radio Access Network (C-RAN) architecture, as shown in Figure 2. In C-RAN, trackside base-band resources conventionally distributed in each base station are now gathered in a Base Band Unit (BBU) pool and scheduled in a centralized way. This removes the need of installing BBU at each RRU location. Hence, reducing the installation cost and facilitating centralized management. From a global perspective, the whole network can be divided into three layers based on their functions, that is, the network control layer centralized at the cloud, the coverage layer formed by sub-6GHz RRUs, and the capacity layer formed by mmWave RRUs.

B) Two-Hop Architecture

Since train carriages are made of metal, severe signal penetration loss is expected of up to 30 dB [14]. For this reason, each User Equipment (UE) is required to increase its transmit power in order to compensate for penetration loss, resulting in greater UE power consumption. Another challenge in this scenario is known as signaling storm in group handover situations, which occurs when many UEs try to handover simultaneously.

To alleviate such problems, a two-hop architecture as depicted in Figure 2 may be an efficient solution. With this architecture, an Access Point (AP) is deployed inside trains to collect passengers' data and then forward the data to trackside base stations through a Mobile Relay (MR) deployed on the outside roof of carriages. In this way, the handover requests are grouped together so that the UEs are seen as a single virtual big UE. This reduces the burden of handover processing and at the same time avoids vehicle penetration losses.

2.3.2 Transport Network

The connection between the RAN and the core network is known as "backhaul". Recently, the development of Cloud-RAN (C-RAN) has given rise to the concept of "fronthaul". A traditional base station (BS) incorporates all the radio and baseband processing functions in the cell site. But the C-RAN architecture splits the traditional BS into two elements: the analog radio-frequency circuitry called Remote Radio Head (RRH), and the Base Band Unit (BBU) that is moved to the cloud (BBU pool or BBU hotel) for centralized signal processing and management. As a result, the idea of "fronthaul" is used to designate the link between the multiple distributed RRHs and the centralized BBU. Although backhaul and fronthaul are different concepts, the term backhaul is generally used to encompass both. Throughout this thesis, we equivalently use BBU/CU/DU to refer to the base band unit and RRH/RRU/RU for distributed radio elements.

There are different technical solutions used by mobile operators for backhaul, including wireline (e.g., copper-line and optic fiber) and wireless solutions (e.g., microwave) [16]. For the rail environment, optical fiber is the preferred choice to provide sufficient bandwidth as well as future capacity expansion for two main reasons. Firstly, optic fiber infrastructure is already available along rail tracks, and further built out is planned. In the second place, IMs and MNOs can make profits from leasing the optical fiber cables to private operators and/or end-users, especially in rural or remote areas where regular and reliable connectivity remains a challenge nowadays.

With C-RAN, traditional complicated cell sites can be converted to cost-effective and power-efficient RRHs by centralizing the processing power. Additionally, centralized processing enables efficient network coordination and management. For instance, the coordination among several RRHs enables inter-cell interference cancellation with coordinated multi-point transmission (CoMP) [17].

Nevertheless, the design of optical fronthaul networks to connect the BBU hotel with the RRHs and to support high-speed fronthaul network traffic is crucial. There still are many topics that are part of current research efforts. Two of the main challenges in optical fronthaul design are explained below.

A) Fronthaul Capacity Bottleneck (CPRI, RoF and Ethernet)

The most common standard used by fronthaul vendors is known as Common Public Radio Interface (CPRI) [18], where the base band I/Q samples are digitized and transmitted at a constant bit rate. Nonetheless, since I/Q streams are oversampled, CPRI transmission needs huge bandwidth for fronthaul networks. For example, for a 100 MHz radio bandwidth and MIMO of order 8, the data rate per sector of the fronthaul transmission system should be of 49.3 Gbps [19], [20].

To address this issue, Radio-over-Fiber (RoF) technology has recently attracted increased interest [21], [22]. In RoF, analog radio frequency signals are sent over optic fiber. This simplifies the interfaces of both BBUs and RRHs, by removing the need of analog to digital (A/D) converters, and at the same time saves bandwidth. Consequently, for the aforementioned scenario, the RoF-based fronthaul just needs 2.4 GHz of bandwidth [23].

Another promising solution to ease the challenging fronthaul data requirements involves redefining the current functional split architecture between the BBU and RRU. Note that in a 5G base station, named gNodeB, the BBU can be further divided into two segments: a Distributed Unit (DU) and a Centralized Unit (CU). The DU is located close to the user, and the CU is located in a data center and virtualized. This leads to a new transport link called "midhaul" that connects the DU to the CU. Figure 3 shows the three parts in which a gNodeB can be divided and the links that connect them, namely fronthaul, midhaul and backhaul.
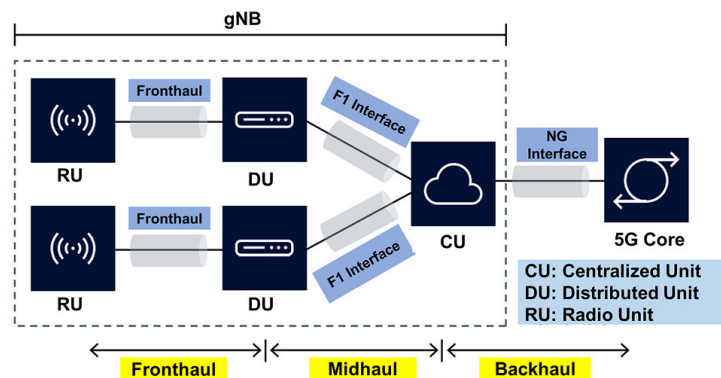
Figure 3 Fronthaul, midhaul and backhaul in 5G [24]

With the approach proposed in [25], the current CPRI architecture is moved towards a packet-based network, such as Ethernet, with new functional splits between BBU and RRU. Ethernet has many advantages including that it allows multiple RRUs to share a common fronthaul resource through virtualization technologies and it also takes advantage of statistical multiplexing, i.e., it allocates bandwidth only to channels that are currently transmitting. Thus, Ethernet provides considerable bandwidth saving compared to CPRI.

In this way, data needs to be encapsulated in the form of packets rather than a constant stream like in CPRI. In a fully centralized C-RAN with a CPRI-like split, the fronthaul data rate is always static and independent of the traffic load, i.e., even if there is no user connected to the RRU, full fronthaul data rates have to be forwarded. However, with a packetized transport network that uses the appropriate RRU-BBU functional split, fronthaul data rate depends on the user traffic. This enables fronthaul data rates to be more closely coupled with the actual user traffic. It has been found that an appropriate functional split could be intra-PHY split, where resource mapping and precoding operations are moved to the RRU instead of being centrally processed at the BBU [25].

B) Ultra-Dense Wavelength Division Multiplexing - Passive Optical Network (u-DWDM-PON)

Another important aspect to take into account is that massive small cell deployment requires a large number of optical fibers. To solve that issue, the High Layer Split (HLS) Dense Wavelength Division Multiplexing Passive Optical Network (DWDM-PON)-based fronthaul solution shown in Figure 4 has been proposed in [26]. HLS relates to the functional split option point in RAN deployments where the interconnectivity point between the CU and the DUs is located in the protocol stack from the MAC layer upwards.

Transmission techniques based on Ultra-Dense Wavelength Division Multiplexing (u-DWDM) are a promising alternative to TDM because of their high spectral efficiency [27]. u-DWDM is implemented by dividing each 100 GHz WDM channel into two sub-channels, one for up-link and the other for down-link, where different user demands can be allocated. In this manner, all antennas linked to the same PON share the same DWDM channel. The advantages of this network design include the coexistence of different traffic types, compatibility with legacy technologies, low congestion at the access nodes, and similar performance to standard dual fiber networks [28], [29].
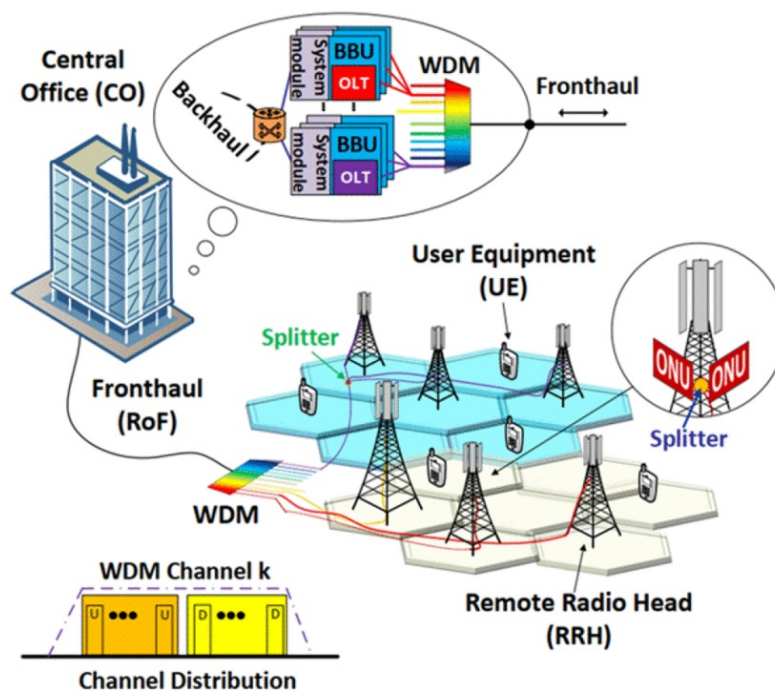

**Figure 4** High-layer split DWDM-PON-based fronthaul solution [22]

C) Network Topology

Following the studies made in [11], [30], the proposed topology for the transport network for FRMCS is similar to the one established for GSM-R.

This architecture is based on two levels:

- National backbone, covering long-distance hops and connected to the core network sites.

- Local/regional rings, dedicated to collecting traffic coming from train stations and rail tracks.

Concerning the second point, a couple of options can be deployed depending on the chosen RAN architecture. In our case, with C-RAN we have separated RRHs at the antenna locations, and "hoteling" of DU/CU (BBU) at edge sites, as illustrated in Figure 5. This design reduces the number of active network components that need to be deployed. RUs are connected to the "centralized" DU/CU in a loop, star or chain.
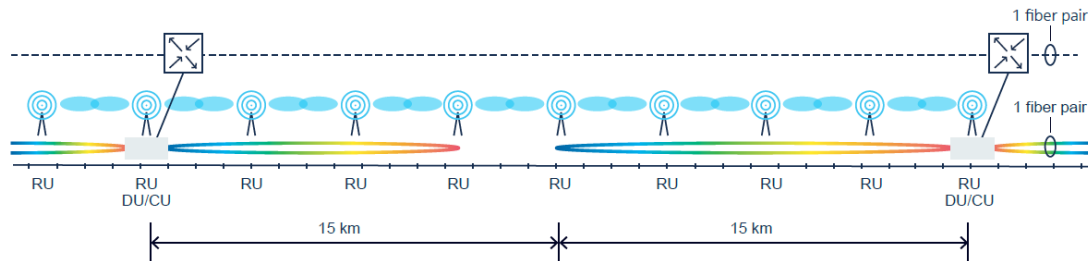
Figure 5 Distributed RUs and hoteling of DU/CU [30]

According to the current latency requirements, a DU/CU hotel can support RUs located up to 15 km away, assuming a maximum fronthaul latency of 100μs given in [31], and deducting 25μs for processing plus a safety margin. The benefit of the design shown in Figure 5 is that the DU/CU pools may be spaced around 24-30 kilometers apart. Nevertheless, the link between the RU and the DU/CU hotel would be lost if the fiber were to be disconnected.

A way to improve availability and reliability is to connect multiple RUs in a loop, as being studied for FRMCS, to connect a single RU to two DU/CU hotels, one acting as main and the other as a backup as shown in Figure 6. In this case, the Inter-Site Distance (ISD) between two DU/CU hotels would be approximately 15 kilometers, meaning that the number of DU/CU hotels needed would be double than in the previous scenario.
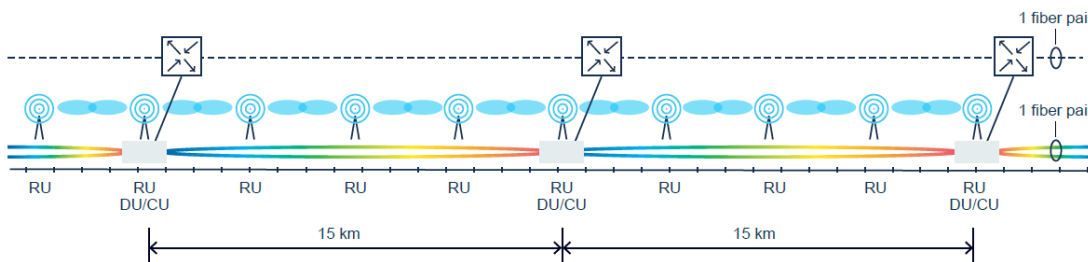

Figure 6 Distributed RUs connected in a loop or to at least two DU/CU hotels [30]

2.3.3 Core Network

The Core Network (CN) design should likewise account for 5G-R services and applications, in which Network Slicing, Software Defined Networking (SDN), and Network Function Virtualization (NFV) concepts are used. A detailed description of network slices suitable for Smart Rail Systems can be found in Section IV of paper [14], where the propagation and channel characteristics for the appropriate frequency bands are considered.

Lastly, Figure 7 shows a complete reference model for the considered 5G/FRMCS solution. On all levels, at least dual redundancy is considered to meet the reliability standards of critical applications that are part of DRO. As we can see, the UE (e.g., cell phone of a passenger or the train in case of DRO) connects to the RUs located along the rail tracks. Then, the optical fronthaul will connect the RUs to the BBU pool located in the train stations. Finally, the optical backhaul will transport the traffic from the BBU pool to the corresponding data center.
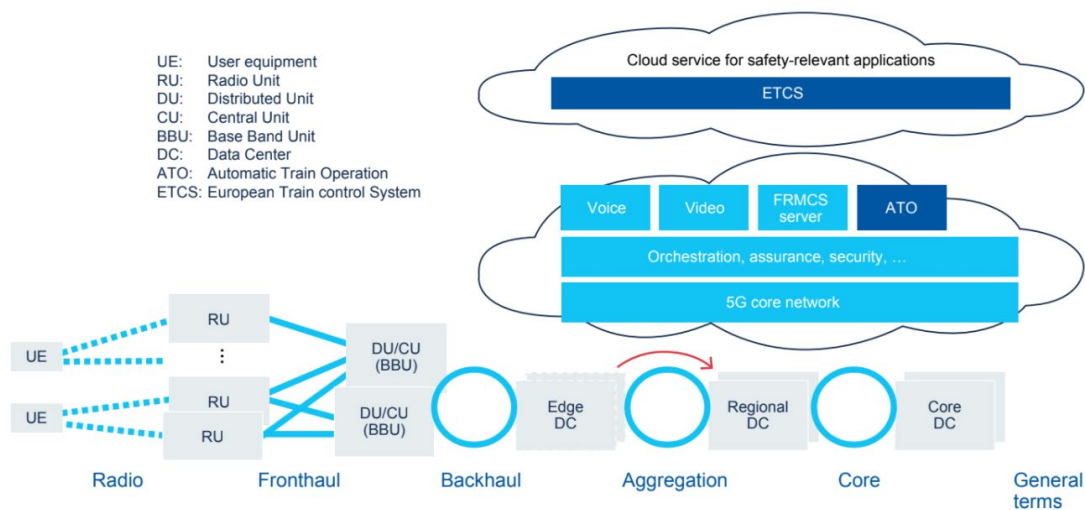
Figure 7 Generic reference architecture [30]

In the case of applications with ultra-low-latency requirements, edge data centers located near the end user are important. Nonetheless, according to the findings in Nokia and Deutsche Bahn's joint White Paper [30], a three-layer separation (edge-regional-core) like the one depicted in Figure 7 is not necessary in the event of typical train operations. This is because the Quality of Service (QoS) parameters for railway use cases can be met with regional and core data centers.

Time sensitive applications will run in regional data centers, where some of the 5G core functions will be distributed. All functionalities of 5G core and other FRMCS components are expected to be housed in two core data centers in a geo-redundant architecture appropriate for disaster recovery. This design is the best trade-off between meeting a railway operator's technical needs and Capital Expenditure/Operational Expenditure (CAPEX/OPEX) according the analysis made in [30].

Chapter 3

Base Station Placement

3.1 Introduction

The Base Station Placement Problem (BSPP) is one of the most important issues to solve when planning a wireless network. This thesis presents an approach to solve the BSPP in the rail environment. The objective is to determine the required number of 5G New Radio (NR) macro and micro base stations, and their location along the rail tracks in order to guarantee a minimum cell edge throughput for the Deutsche Bahn's long-distance railway system in Germany.

A) Related Work

The ETSI TR 103 554-2 was released in February 2021 [32]. The purpose of this Technical Report (TR) is to evaluate 3GPP NR radio performance in the rail scenario since NR is one of the candidates for the radio access technology to be utilized in FRMCS. The paper defines many scenarios for different radio conditions that are common in the rail environment, in the 900 MHz (FDD, 5 MHz bandwidth) and the 1900 MHz bands (TDD, 10 MHz bandwidth). Inter-site distances (ISD) between 2 km and 8 km were evaluated in system simulations by three different companies.

The majority of the document focuses on the results and analysis of a comprehensive system simulation campaign conducted by the three companies using similar input assumptions but different modeling and simulation approaches. Some of the parameters that differed in each company's simulation include MIMO, Doppler, uplink power control target or target minimum coupling loss, which resulted in a wide variance in some simulation scenarios. The participating firms also considered a variety of interference mitigation strategies such as no mitigation, interference rejection based on channel knowledge and frequency reuse.

The study indicates that the throughput performance of the uplink, i.e., from train to ground infrastructure, is the limiting factor in the radio deployment in rail environments for DRO applications. Furthermore, the findings reveal that under railway scenarios, throughput performance is primarily interference limited, and that the use of interference mitigation techniques such as those provided by 5G NR is crucial. However, due to the high variance of the achieved throughputs in the simulations by the three companies, the authors conclude that the results outlined in the TR are just indicative and detailed design criteria for rail deployments cannot be reached.

B) Assumptions

To simplify the deployment scenario, a series of assumptions will be made based on the proposed network architecture described in Section 2.3 of this thesis.

- Each macro cell will be composed of:

  1- One sub-6GHz RRH operating in the 1900 MHz band, giving omnidirectional coverage and supporting the control signaling of passenger connectivity (with C/U-decoupling), and DRO services under FRMCS (without C/U-decoupling).

  2- A number of mmWave RRHs operating in the 30 GHz band, that will be associated to the macro BS, in charge of providing high data rates for passenger connectivity U-plane.

- Each macro cell must meet the minimum requirements of the train-control and passenger-oriented connectivity services using the heterogeneous deployment with sub-6GHz and mmWave RRHs. In the case of DRO, the throughput requirement is stricter in the uplink (UL) than in the downlink (DL). Therefore, the UL will be the limiting link. We assume that the DL throughput requirements will always be met in the link budget calculation, i.e., for DRO we will only calculate the link budget for the UL. For passenger connectivity, the DL will be the limiting case since it has the strictest requirements. Thus, we assume that the UL throughput requirements will always be met since the transmit power of the user terminal on top of the train carriage is greater than the mmWave RRH's transmit power.

- We consider that each train station will host a macro base station and a BBU hotel. In some cases, the distance between the RRH and the closest train station, that will host the BBU pool, will be longer than the maximum fronthaul distance of 15 km stated in Section 2.3.2. In this situation, some of the macro base stations located in the middle of the link between two train stations will also be able to host BBU pools. The optimal placement of BBU pools is another network planning problem, but it will not be researched in this thesis.

- The C-RAN architecture facilitates the coordination among several RRHs, which enables inter-cell interference cancellation with coordinated multi-point transmission (CoMP). Thus, the inter-site interference is not considered in the calculations and the Signal-to-Noise-Ratio (SNR) is used interchangeably with the Signal-to-Interference-plus-Noise-Ratio (SINR) throughout the thesis.

- The planning of the placement of base stations along the rail tracks will be made using a link budget calculation approach with our proposed algorithm. Using a professional planning tool is out of scope due to time and resource constraints.

C) Limitations of Link Budget vs Planning Tool

Finding a rough estimate of the required number of 5G base stations in a certain area is an initial but critical step for the planning and implementation of a 5G network. It is an important pre-sales activity for network operators because it will help them to estimate the necessary investments and effort in their business plans.

By using the link budget computation, we can determine the achieved capacity based on several parameters such as the Signal-to-Interference-plus-Noise Ratio (SINR). However, it is not realistic to design a network on the sole basis of link budget calculation and ignoring the use of network planning tools like Planet or Atoll since the link budget computation will not deliver the coordinates of cell sites.

The propagation model utilized is the most important aspect in both calculations (link budget and planning tool). The cell radius will be different even if the same propagation model is used in the link budget and the planning tool. This is because the planning tool makes complex calculations based on the topography of the terrain, clutter and other parameters like reflection, refraction and attenuation caused by obstacles (trees, buildings, rain, etc.). Additionally, in order to determine the network performance (user throughput, cell load, capacity, etc.), the support of Monte Carlo simulations by the planning tool is crucial but it is also more time consuming and more detailed inputs are required [33].

Nevertheless, the outputs obtained from link budget calculation can be used as inputs for the planning tool. Thus, the approach that is proposed in this thesis to solve the BSPP, which is based on link budget calculation, can be considered as an approximation of the required number of BSs. The main outputs will be the cell radius, required number of 5G NR base stations and achieved throughput at cell edge.

3.2   System Model

This section describes the deployment scenario considered for the BSPP.

A) Channel Model

We use the rural macro (RMa) model specified in 3GPP TR 38.901 [34]. This model is designed for macro cell scenarios, which are characterized by having larger ISDs and low building density. Because train antennas are located outside the train carriage, the penetration loss present in the RMa Non-Line-of-Sight (NLOS) model is removed and only the Line-of-Sight (LOS) is taken into account. The RMa propagation model is also used for the micro base stations since it is valid for a frequency range from 0.5 to 100 GHz.

The path loss follows the formula described in Table 3.

Path loss (dB)	Shadow fading std (dB)	Applicability range
$PL = \begin{cases} PL_1, & 10m \leq d_{2D} \leq d_{BP} \\ PL_2, & d_{BP} \leq d_{2D} \leq 10km \end{cases}$ $PL_1 = 20log_{10}\left(40\pi d_{3D}\frac{f_c}{3}\right) + \min(0.03h^{1.72},10)\,log_{10}(d_{3D})$ $- \min(0.044h^{1.72},14.77)$ $+ 0.002log_{10}(h)d_{3D}$ $PL_2 = PL_1(d_{BP}) + 40log_{10}\left(\frac{d_{3D}}{d_{BP}}\right)$	$\sigma_{SF} = 4$ $\sigma_{SF} = 6$	$5m \leq h \leq 50m$ $10m \leq h_{BS} \leq 150m$ $1m \leq h_{UT} \leq 10m$ $0.5 \leq f_c \leq 100GHz$

Table 3 Propagation model [34]

Where d_{2D} is the 2D-distance, d_{BP} is the break-point distance, d_{3D} is the 3D-distance, f_c is the carrier frequency in GHz, and h is the average building height. All the distances are given in meters. Figure 8 depicts the defined distances in the propagation model.
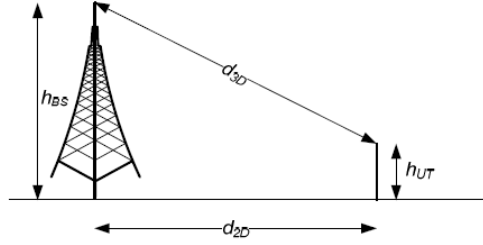
Figure 8 Definition of d2D and d3D for outdoor UTs [34]

Note that $d_{3D} = \sqrt{d_{2D}^2 + (h_{BS} - h_{UT})^2}$

The break-point is defined as $d_{BP} = 2\pi \cdot h_{BS} \cdot h_{UT} \cdot \frac{f_c}{c}$, where f_c is the center frequency in Hz, $c = 3 \cdot 10^8$ m/s is the propagation velocity in free space, and h_{BS} and h_{UT} are the antenna heights at the BS and the UT, respectively.

B) Notation

Table 4 describes the notation used in the BSPP.

Parameter	Definition
f_c	Carrier frequency
B	Bandwidth
PL	Path loss
L_{rain}	Rain loss
$L_{foliage}$	Foliage loss
L	Total losses including path, rain and foliage
$P_{T,UT}$ - $P_{R,UT}$	Transmitted power and nominal received power by the user terminal
$P_{T,BS}$ - $P_{R,BS}$	Transmitted power and nominal received power by the base station
$P_{N,BS}$, $P_{N,UT}$	Noise power at the base station and at the user terminal
$G_{T,UT}$ - $G_{R,UT}$	Transmit and receive user equipment antenna gain
$G_{T,BS}$ - $G_{R,BS}$	Transmit and receive base station antenna gain
SNR_{nom}	Nominal Signal-to-Noise Ratio
k	Boltzmann constant, k= $1.38 \cdot 10^{-23}$ J/K
T_0	Equivalent noise temperature, T=290K

F_{UT}, F_{BS}	Noise figure of user terminal and base station, respectively
A_f	Slow fading
MF	Fade margin
$P_{r,UT}$	Local average received power by the user terminal
$P_{r,BS}$	Local average received power by the base station
SNR_{min}	Minimum average received Signal-to-Noise Ratio

Table 4 Notation used in the BSPP

C) Network representation using a graph

Deutsche Bahn's long-distance rail system is represented using an undirected and edge-weighted graph denoted as $G(N,E)$, where N is the set of nodes and E is the set of edges or links. The nodes represent the train stations and the edges are the connections between two train stations if a route exists between those stations. The weights or costs of the edges are the Euclidean distance between the two train stations in a 2D map projection. A representation of the complete long-distance rail system being considered is shown in Figure 9.


Figure 9 Rail network representation

The dataset that is used in this thesis was obtained from the General Transit Feed Specification (GTFS) for Germany [35]. This website offers daily generated timetable datasets in the GTFS format covering the complete long-distance and regional rail network of Deutsche Bahn as well as local/urban transit of all agencies and companies in Germany. In our case, only the Long-Distance Rail dataset was used. This dataset spans over a week and has a minute granularity. The statistics listed in Table 5 have been obtained from the aforementioned dataset.

Parameter	Value
Number of train stations	304
Number of links	554
Min. link length	332 m
Max. link length	309.3 km
Avg. link length	45.3 km
Max. num. of trains in a link	8 trains/link
Max. num. of active trains per minute	289 trains
Avg. num. of active trains per minute	166 trains
Min. train speed	5 km/h
Max. train speed	272 km/h
Avg. train speed	98 km/h
Max. density (all links)	3 trains/km
Max. density (links > 10 km)	0.5 trains/km
Avg. density	0.1 trains/km

Table 5 Statistics of the rail network

Figure 10 illustrates a histogram describing the utilization of rail links. As observed, there are 4 links that have a maximum of 8 active trains circulating simultaneously in a minute. Nevertheless, around 80% of the links only have between 1 and 2 trains circulating at the same time.
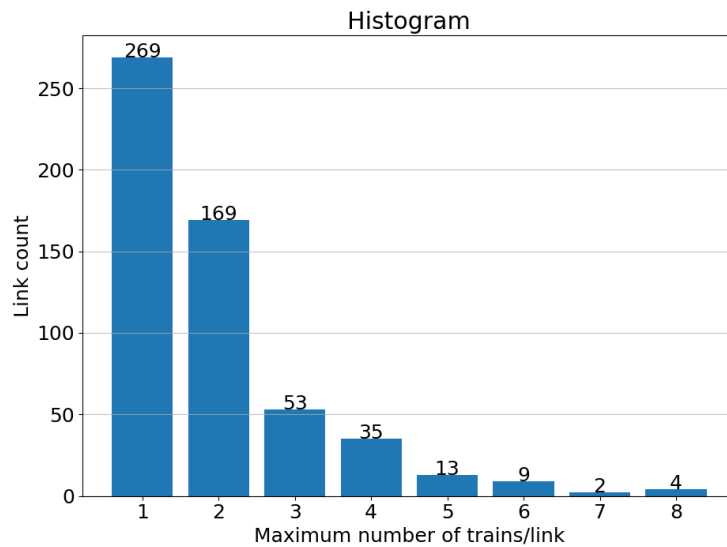

Figure 10 Histogram maximum number of trains per link

D) Deployment scenario

We assume a rail system with two parallel long-distance tracks (rural scenario) with specified inter-track distance of 6 m. A linear deployment along the railway line is expected with a macro base station tower to track distance of 15 m as shown in Figure 11 and a RRH to track distance of 5 m for the micro base station as depicted in Figure 12.
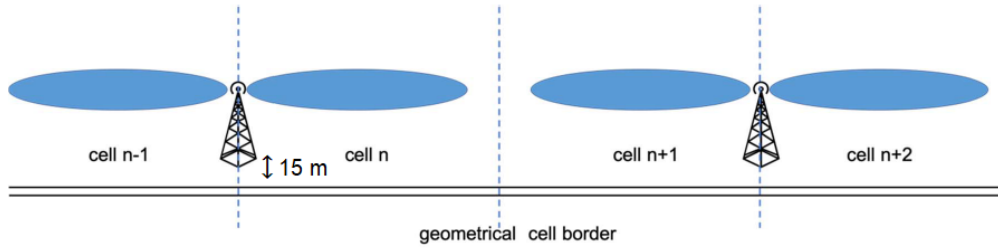
Figure 11 Macro cellular network layout [32]
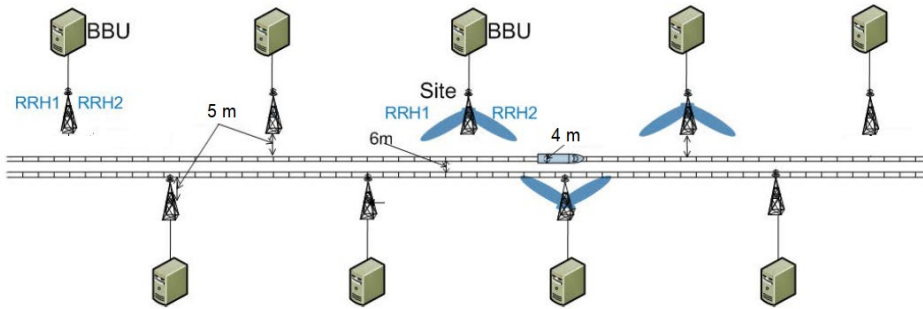
Figure 12 Micro cellular network layout [36]

3.3   Implementation

A) Link Budget

We first determine the coverage radius of the macro and micro base stations as a function of the required cell edge throughput by means of the link budget calculation.

A.1) Macro Base Station

The deployment parameters for the macro base station are detailed in Table 6.

RMa @ f_c = 1900 MHz (TDD, B = 10 MHz)	
Input data	DL/UL Ratio: 10/90
	Numerology - Subcarrier Spacing (μ): (1:30 kHz)
	f_c = 1900 MHz
	Max number of PRB (Physical Resource Block): 24
gNodeB configuration	Transmit power: 40 or 63 dBm
	Antenna gain: 18 dB
	Antenna height: 35 m
	Noise figure: 4 dB
UT configuration	Transmit power: 31 dBm
	Antenna gain: 0 dB
	Train antenna height: 4 m
	Noise figure: 6 dB
5G Propagation Model (3GPP 38.901)	3D-RMa LOS
Additional losses	Typical foliage loss: 11 dB
	Rain/Ice margin: 0 dB
	Type of coverage: outdoor

Table 6 Deployment parameters macro BS

Link Budget (Uplink: UT→BS)

The received power by the macro base station can be written as:

$$P_{R,BS} = \frac{P_{T,UT} G_{T,UT} G_{R,BS}}{L}, \qquad L(dB) = PL(dB) + L_{rain}(dB) + L_{foliage}(dB) \qquad \textbf{(1)}$$

$$P_{R,BS}\ (dBm) = 31\ dBm + 0\ dB + 18\ dB - PL\ (dB) - 11\ dB - 0\ dB$$
$$= 38\ dBm - PL(dB)$$

where $P_{T,UT}$ is the UT transmit power, $G_{T,UT}$ and $G_{R,BS}$ are the antenna gains at the UT and BS sides, respectively, and L is the total loss including path loss (PL), rain loss (L_{rain}) and foliage loss ($L_{foliage}$).

The noise power is:

$$P_{N,BS} = kT_o F_{BS} B, \qquad P_{N,BS}(dBm) = -174\frac{dBm}{Hz} + F_{BS}(dB) + 10 \cdot \log(B) \qquad \textbf{(2)}$$

$$P_{N,BS}(dBm) = -174 + 4 + 10 \cdot \log(10 \cdot 10^6) = -100\ dBm$$

where k is the Boltzmann constant, F_{BS} is the noise figure in the BS, and B is the bandwidth.

The nominal SNR in the BS is equal to the received power in Equation (1) divided by the noise power in Equation (2).

$$SNR_{nom} = \frac{P_{R,BS}}{P_{N,BS}}, \qquad SNR_{nom}(dB) = P_{R,BS}(dBm) - P_{N,BS}(dBm) \qquad \textbf{(3)}$$

$$\boldsymbol{SNR_{nom}(dB)} = 38\ dBm - PL(dB) + 100\ dBm = \mathbf{138} - \boldsymbol{PL(dB)}$$

A high SNR or SINR value can help to achieve higher spectral efficiency since it enables to decode higher Modulation Coding Schemes (MCS). SINR is also measured to express the relationship between radio conditions and throughput. For instance, it can be used to calculate the Channel Quality Indicator (CQI) value [37]. The CQI is typically represented as a data rate that the user terminal (UT) can handle under current radio conditions rather than as a received signal quality. The MCS parameter can then be assigned based on the CQI value. Specific implementations for the CQI and MCS values as well as SNR to CQI mapping are usually vendor-specific. In LTE, the CQI has 15 codes and up to 22.7 dB of SINR. In this thesis, we use MCS mappings from [38] for 5G NR, which correspond to 128 codes with a maximum SNR of 40 dB.

Finally, according to Shannon's capacity theorem, the theoretical capacity (C) of an ideal Additive White Gaussian Noise (AWGN) channel is a function the channel bandwidth and the SNR. From this theorem, the following upper bound for the bit rate can be derived.

$$R_b \leq C = 0.9 \cdot B \cdot \log_2(1 + SNR) \qquad \textbf{(4)}$$

$$\boldsymbol{R_b \leq 0.9 \cdot 10 \cdot \log_2\left(1 + 10^{\frac{138 - PL(dB)}{10}}\right) [Mbps]}$$

Note that a 0.9 penalty has been added in order to take into account the UL/DL ratio since the R_b value corresponds to the UL throughput. Finally, the base station coverage radius can be derived from the previous equation, where the path loss $PL\ (dB)$ can be found to guarantee a given cell edge throughput R_b.

A.2) Micro Base Station

The same procedure can be used to determine the coverage radius and cell edge throughput for the micro BS. In this case, the downlink (DL) is considered as the limiting link, as stated in the assumptions of Section 3.1 B). The deployment parameters for the micro base station are detailed in Table 7.

RMa @ f = 30 GHz (B= 800 MHz with carrier aggregation)	
Input data	DL/UL ratio: 50/50
	Numerology - Subcarrier Spacing (µ): (3:120 kHz)
	f_c = 30 GHz
	Max. number of PRB: 264 + 264 = 528
gNodeB configuration	Transmit power: 35 dBm
	Antenna gain: 15 dB
	Antenna height: 10 m
	Noise figure: 4 dB
UT configuration	Transmit power: 31 dBm
	Antenna gain: 0 dB
	Train antenna height: 4 m
	Noise figure: 6 dB
5G Propagation Model (3GPP 38.901)	3D-RMa LOS
Additional losses	Foliage loss: 0 dB
	Rain/Ice margin: 3 dB
	Type of coverage: outdoor

Table 7 Deployment parameters micro BS

Link Budget (Downlink: BS→UT)

The received power by the user terminal can be written as:

$$P_{R,UT} = \frac{P_{T,BS}G_{T,BS}G_{R,UT}}{L}, \qquad L(dB) = PL(dB) + L_{rain}(dB) + L_{foliage}(dB) \tag{5}$$

$$P_{R,BS}\,(dBm) = 35\,dBm + 15\,dB + \,0\,dB - PL\,(dB) - 3\,dB - 0dB$$
$$= 47\,dBm - PL(dB)$$

The noise power is:

$$P_{N,UT} = kT_oF_{UT}B, \qquad P_{N,UT}(dBm) = -174\frac{dBm}{Hz} + F_{UT}(dB) + 10 \cdot \log(B) \tag{6}$$

$$P_{N,UT}(dBm) = -174 + 6 + 10 \cdot \log(800 \cdot 10^6) = -79\,dBm$$

The nominal SNR in the UT is equal to the received power divided by the noise power.

$$SNR_{nom} = \frac{P_{R,UT}}{P_{N,UT}}, \qquad SNR_{nom}(dB) = P_{R,UT}(dBm) - P_{N,UT}(dBm) \tag{7}$$

$$\boldsymbol{SNR_{nom}(dB)} = 47\,dBm - PL(dB) + 79\,dBm = \boldsymbol{126 - PL(dB)}$$

Lastly, Shannon's channel capacity formula is used again to determine the bit rate in the downlink. Note that in this case the DL/UL ratio is 50/50. That is why a penalty of 0.5 is added to the formula.

$$R_b \leq C = 0.5 \cdot B \cdot log_2(1 + SNR) \tag{8}$$

$$\boldsymbol{R_b \leq 0.5 \cdot 800 \cdot log_2\left(1 + 10^{\frac{126 - PL(dB)}{10}}\right)[Mbps]}$$

B) Placement of Base Stations

Having the equations for determining the coverage radius of the macro and micro BS, the next step consists in integrating these in the algorithm used for solving the BSPP problem. This algorithm was written using Python 3.8.8 and its library for graphs NetworkX. The pseudocode for BSPP subroutines is presented in the following code listings.

---

def split(start, end, segments):

Objective: Function to split a straight line, with a start and end coordinates, in a sequence of segments.
Input: Start coordinates, end coordinates, number of segments.
Output: List containing the coordinates of the division points, and length of a segment.

---

def place_BS_macro(start, end, req_throughput, link_distance):

Objective: Function to place the macro base stations in a train link given the coordinates of the two stations (start and end), the required cell edge throughput and the length of the link.
Input: Start coordinates, end coordinates, required cell edge throughput, distance of the link.
Output: List containing the coordinates of the macro BS, distance between two macro BS.

---

def place_BS_micro(start, end, req_throughput, link_distance):

Objective: Function to place the micro base stations in a train link given the coordinates of the two stations (start and end), the required cell edge throughput and the distance of the link.
Input: Start coordinates, end coordinates, required cell edge throughput, distance of the link.
Output: List containing the coordinates of the micro BS, distance between two micro BS.

---

def micro_in_macro_radius(pos_macro, pos_micro, radius):

Objective: Function to cluster the micro BSs to a macro BS. It determines if the micro BS is in the coverage area of the macro BS.
Input: position of the macro BS, position of the micro BS, radius of coverage of the macro BS
Output: Boolean (True or False)

Lastly, the BSPP algorithm that has been used in this thesis is described below.

Algorithm 1: Base Station Placement and Clustering

1:	Create dataframe from csv file of the GTFS using Pandas
2:	Create graph G(N,E) with train stations and links using NetworkX
3:	**for** each edge E in graph G(N,E)
4:	get "start" and "end" coordinates of the train stations from E's attributes
5:	call macro_BS_list = place_BS_macro(start, end, req_throughput_1, link_distance)
6:	call micro_BS_list = place_BS_micro(start, end, req_throughput_2, link_distance)
7:	**for** each macro base station "pos_macro" coordinate in macro_BS_list
8:	add new macro base station node "MBS" to G(N,E)
9:	**if** it is the first MBS of the current edge E **then**
10:	add edge(start, pos_macro) to G(N,E)
11:	**else**
12:	add edge(pos_macro-1, pos_macro) to G(N,E)
13:	**end if**
14:	**if** it is the last MBS of the current edge E **then**
15:	add edge(pos_macro, end) to G(N,E)
16:	**end if**
17:	**for** each micro base station "pos_micro" coordinate in micro_BS_list
18:	call condition = micro_in_macro_radius(pos_macro, pos_micro, radius)
19:	**if** condition is True **then**
20:	add traffic of pos_micro to pos_macro /*Clustering*/
21:	remove pos_micro from micro_BS_list
22:	**end if**
23:	**end for**
24:	**end for**
25:	**end for**

Input: GTFS dataset, req_throughput_1 (for the macro BS), req_thorughput_2 (for the micro BS)

Output: Graph *G(N,E)* where *N* is the set of train stations and macro BSs and *E* is the set of edges. Each macro BS aggregates its own traffic and the one of the clustered micro BS.

Note that in Algorithm 1, only the macro BS nodes are added to the graph *G(N,E)* since the number of micro BSs that are needed for the whole rail network is too large. In the case of the micro BS, a clustering is made using the *micro_in_macro_radius* function. This means that the number of micro BSs that are needed for each link is computed and then each micro BS is associated to its closest macro BS.
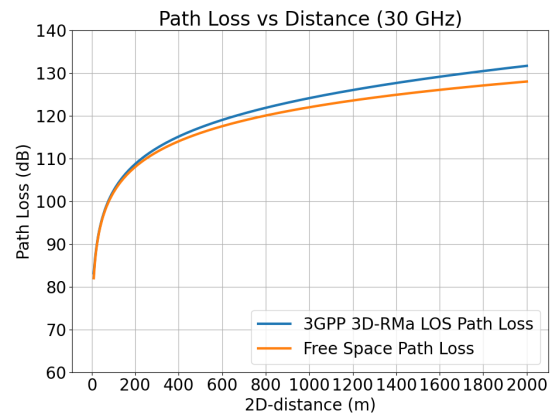
3.4 Results

The results obtained using Algorithm 1 for solving the BSPP are presented next.

### A) Link Budget
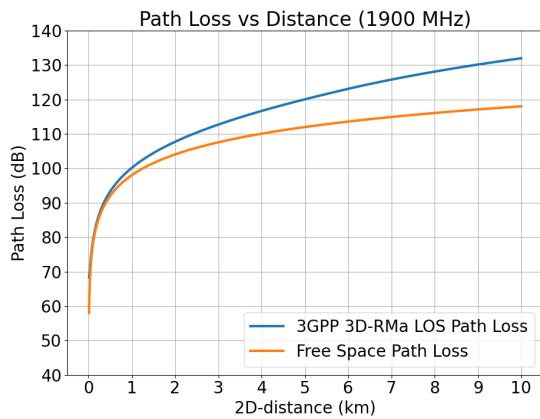
Figure 13 Path loss 1900 MHz

Figure 14 Path loss 30 GHz

Figure 13 shows the path loss computation using the macro base station parameters from Table 6 and the RMa LOS model described in Table 3. The orange line depicts the free space path loss based on Recommendation ITU-R P.525-4 [39]. While the blue line shows the path loss using the 3GPP 3D-RMa LOS model. As we can observe, the path loss using the two models is very similar for small distances, but as the distance increases the divergence between the lines grows.

Figure 14 depicts the path loss for the micro base station using the parameters of Table 7, also for the RMa LOS model and the free space path loss. Since the carrier frequency in this case is higher, the path loss increases faster than in the macro base station scenario.
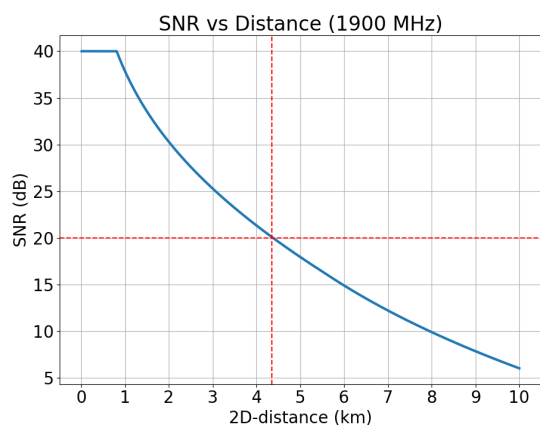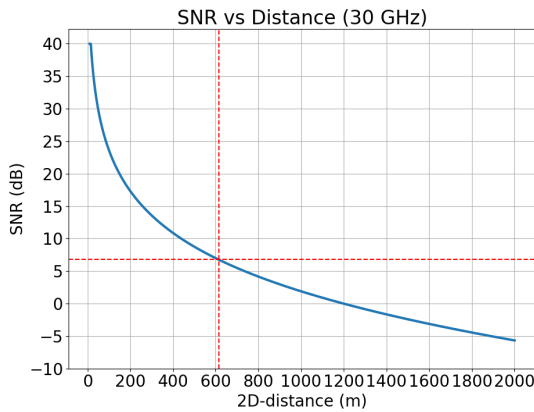

Figure 15 Nominal SNR macro base station
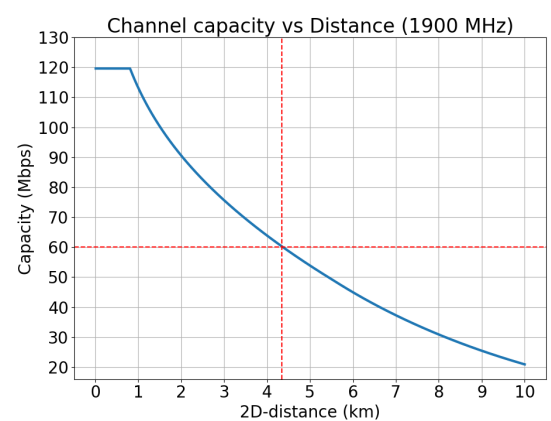
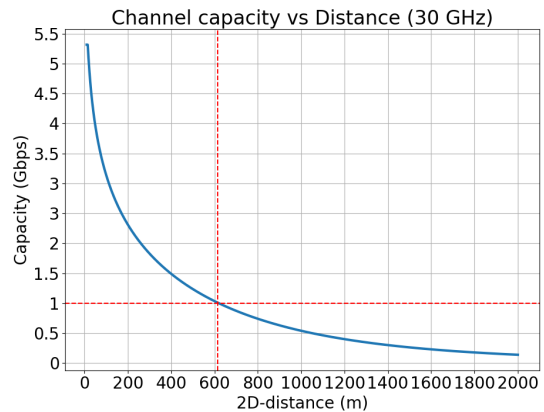**Figure 16** UL data rate macro base station

Following the procedure explained in Section 3.3 A), the nominal SNR at the macro base station can be obtained using Equation (3). The result is represented in Figure 15 with a maximum SNR of 40 dB up to 800 m and a minimum of 6 dB at 10 km. These

29

SNR values are quite high since the UT is not a common cell phone, but a mobile relay located on top of the train carriage. Furthermore, we have not added the effect of slow fading (shadowing) in the SNR. This effect will be explained in Section 4.3 D).

The uplink bit rate at the macro BS is computed using Shannon's capacity theorem described in Equation (4) and its result is shown in Figure 16. For DRO applications, a minimum requirement of 15 Mbps per train is expected for the uplink according to Table 1. Considering a macro BS has to give service to 4 trains at the same time in the worst case (two trains in each direction), a cell radius of 4.35 km is obtained to guarantee 60 Mbps of cell edge throughput.

**Figure 17** Nominal SNR micro base station

Figure 18 DL data rate micro base station

Figure 17 represents the nominal SNR at the UT for the micro base station scenario using Equation (7). In this case, the SNR drops faster than in the previous case (macro base station) since the frequency is much higher. Around 1.2 km, the SNR reaches 0 dB (same strength of desired signal and noise) and a minimum of -5 dB around 2 km. Consequently, the downlink bit rate, at the UT, also drops very quickly as seen in Figure 18 which follows Equation (8). As it was shown in Table 2, by 2030, the forecasts predict a traffic demand of 1 Gbps per train for passenger connectivity. Thus, a coverage radius of 610 m is advised for the micro BS assuming it has at most one train to service.
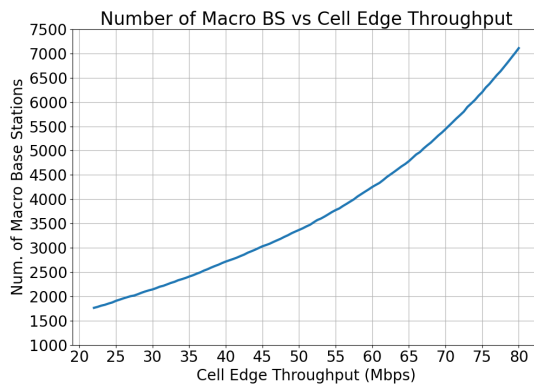
B) Placement of Base Stations

Figure 19 depicts the result for the base station placement computed using Algorithm 1. In the diagram, cyan nodes represent the train stations and yellow nodes are the macro base stations. The micro base stations are not shown to improve the visibility since the number of micro BSs by far exceeds the number of macro BSs.

Using this approach, it has been calculated that 4,252 macro base stations with an ISD of 8.3 km and 31,616 micro base stations with and ISD of 1.1 km are needed to guarantee 60 Mbps of cell edge throughput in the macro BS and 1 Gbps of cell edge throughput in the micro BS.
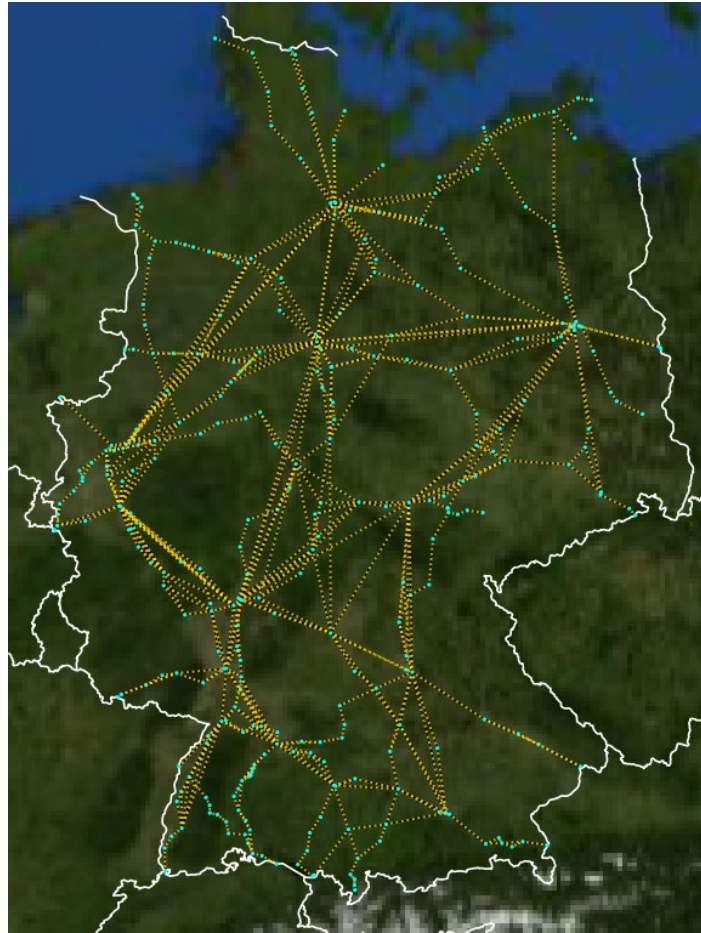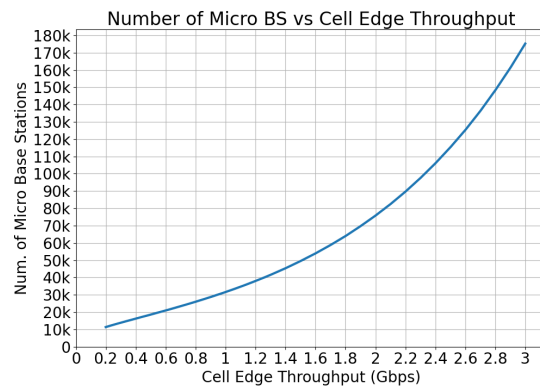
Figure 19 Network topology with macro base stations

C) Sensitivity analysis

Figure 20 Sensitivity analysis on the number of macro base stations

Figure 21 Sensitivity analysis on the number of micro base stations

After the placement of the BSs, a sensitivity analysis was made in order to evaluate the scalability of the network in the future with stricter throughput requirements. Figure 20 and Figure 21 portray how the number of macro and micro base stations, respectively, vary in function of the cell edge throughput requirement. Both graphs follow an exponential-like behavior, in which the number of necessary BSs rapidly increases for larger bandwidth demands.

D) Fade margin and MIMO

All the previous results have been obtained using an optimistic value of the SNR, as explained in Section 3.3, since the slow fading has not been taken into account. Slow fading is caused by shadowing, which is the deviation of the power of the received electromagnetic signal from an average value (nominal SNR) due to obstacles affecting the wave propagation, vegetation or terrain characteristics. The calculations and graphs depicting the SNR and the bit rate when considering the effect of the slow fading can be found in Appendix A. There, the use of Multiple-Input Multiple-Output (MIMO) technology is also introduced.

Chapter 4

Data Center Placement and Assignment

4.1   Introduction

A data center (DC) is a facility used to house an organization's IT systems and equipment. It enables the storage, processing, and delivery of data and applications [40]. This part of the bachelor's thesis aims to find the required number of data centers and their location, and to assign them to each train station in the long-distance railway system of the Deutsche Bahn. We call this the Data Center Placement and Assignment Problem (DCPAP). In addition, this section will also cover the routing sub-problem derived from the Routing and Wavelength Assignment (RWA) problem. In this case, it consists on finding the route for the connection between a train station (source) and its assigned data center (destination).

The RWA problem is a typical optimization problem in optical networks. Given a set of connections between node pairs in an optical network, the objective is to set up a light path for each connection by assigning a route, i.e., a sequence of physical links from source to destination, and a wavelength to be employed for every connection. The RWA problem is a very complex problem (NP-complete) [41]. Integer Linear Programming (ILP) formulations may be utilized to jointly find the optimal solution for both routing and wavelength assignment. However, due to the complexity of solving large instances, the problem is usually split in two sub-problems: the routing sub-problem and the wavelength assignment sub-problem.

4.2   System Model

The first step was to identify potential data center locations for the network to use as an input for the DCPAP. For that, the Germany50 dataset was extracted from SNDlib [42]. It is a library of test instances for "Survivable fixed telecommunication Network Design". This dataset contains the nodes and links of Germany's core network with a total of 50 potential data center locations for the DCPAP and is represented in Figure 22.

Then, a mapping between the potential data center locations and the closest train station was conducted to build the network topology. We model the system using graph *G(N,E)*, which was used in the BSPP. The system model is depicted in Figure 23. Cyan nodes represent train stations and red nodes are potential data center locations, which at the same time, are train stations of the network. The links of the core network are shown in orange to differentiate them from the links of the rail network, represented in black.

Figure 22 Germany50 dataset representation [42]

Figure 23 Graph with train stations and potential DC locations

Another input parameter needed for the DCPAP are the bandwidth demands of the train stations that will be processed in the data centers. In order to define the traffic demands, the worst-case scenario is considered. This means the maximum number of trains simultaneously circulating in each link of the rail network, as previously shown in Figure 10. We assume that the aggregated bandwidth demand, generated by all the trains running on a link, is symmetrically distributed (50:50) to the source and destination train stations of the given link. Figure 24 illustrates a histogram with the bandwidth demands per train station. Around 60% of the train stations demand less than 3 Gbps. The aggregated demand of all train stations is 1,087,402 Mbps with a maximum demand per train station of 34 Gbps.

Figure 24 Histogram for the bandwidth demand by train station

34

4.3 Problem Formulation

We model the Data Center Placement and Assignment Problem (DCPAP) using an Integer Linear Programming (ILP) formulation. The ILP-based optimization model returns the optimal placement of data centers, and the assignment of a data center to each train station. The goal is to minimize the latency and Operational Expenditures (OPEX), i.e., the monthly cost of leasing optic fiber cables for the backhaul and data centers. Regarding the routing sub-problem, the shortest-path routing approach is selected as it was done in [43]. The shortest-path route is pre-calculated offline using Dijkstra's algorithm for each train station and potential data center pair.

In other words, the problem's objective is to determine a subset C' from the set of potential data center nodes C that minimizes the latency and the cost of infrastructure leasing, and to assign a data center to each train station. Table 8 describes the notation of the input and output parameters used in the ILP problem formulation.

Symbol	Description
Input parameters	
N : $\{N_1, N_2, ..., N_n\}$, $n \in \mathbb{Z}^+$	Set of all nodes (train stations), in the graph. Some train stations are also potential data center locations.
E : $\{E_1, E_2, ..., E_m\}$, $m \in \mathbb{Z}^+$	Set of all links in the network.
C : $\{C_1, C_2, ..., C_p\}$, $p \in \mathbb{Z}^+$, $C \subseteq N$	Set of all potential data center nodes in the topology. C is a subset of N. All potential data centers are also train stations, but not all train stations are potential data centers.
B : $\{B_1, B_2, ..., B_n\}$, $n \in \mathbb{Z}^+$	Set of train stations' aggregated bandwidth demands, in Mbps.
U_e, $\forall e \in E$	Bandwidth capacity, in Mbps, of optical link e.
V_c , $\forall c \in C$	Bandwidth capacity, in Mbps, of potential data center c.
T	Maximum tolerated latency, in ms.
K	Maximum number of data centers that can be located in the network.
$sp(n,c)$, $\forall n \in N$, $\forall c \in C$	Propagation delay for the shortest path from train station n to data center c.
$S(n,c)$, $\forall n \in N$, $\forall c \in C$	Set of edges for the shortest path from train station n to data center c.
$d(n,c)$, $\forall n \in N$, $\forall c \in C$	Total latency from train station n to data center c.
p_e	Cost of leasing the optic fiber infrastructure for edge e in EUR/Mbps.
p_c	Cost of leasing data center c in EUR/month.
Output parameters	
$x(n,c)$, $n \in N$, $c \in C$	Binary variable that equals 1 if train station n is assigned to data center c.
$y(e,n,c)$, $e \in E$, $n \in N$, $c \in C$	Binary variable that equals 1 if link e is used to connect train station n to its assigned data center c.
δ_c, $c \in C$	Binary variable that equals 1 if data center c is selected by at least one train station.
C': $\{ C'_1, C'_2, ..., C'_{K'}\}$, $K' \leq K$	Set of data centers that will be used in the network.
K'	Number of data centers that are used.

Table 8 DCPAP Problem formulation parameters

The objectives and constraints of the ILP are described below.

Latency minimization objective: Minimizes the latency for the connection between a train station and its assigned data center.

$$\min z_d = \sum_{n \in N} \sum_{c \in C} (x(n,c) \cdot d(n,c)) \tag{9}$$

Cost minimization objective: Minimizes the OPEX, i.e., cost of renting the infrastructure. That is data centers and optic fiber along the rail tracks.

$$min\ z_c = \sum_{c \in C} (\delta_c \cdot p_c) + \sum_{e \in E} \sum_{n \in N} \sum_{c \in C} (y(e,n,c) \cdot B_n \cdot p_e) \tag{10}$$

Bi-objective optimization: Minimizes the weighted sum of the two objectives, α and β being the associated weights.

$$min\ (\alpha \cdot z_d + \beta \cdot z_c) \tag{11}$$

Data center capacity constraint: The aggregated bandwidth assigned to data center c must be kept at, or below, c's bandwidth processing capacity.

Subject to:

$$\sum_{n \in N} (x(n,c) \cdot B_n) \le V_c , \forall c \in C \tag{12}$$

Link capacity constraint: The aggregated bandwidth passing through optical link e must be kept at, or below, e's link bandwidth capacity.

Subject to:

$$\sum_{n \in N} \sum_{c \in C} (y(e,n,c) \cdot B_n) \le U_e, \forall e \in E \tag{13}$$

Latency constraint: The latency in the connection between train station n and its assigned data center c must be equal, or below, an upper bound T.

Subject to:

$$\sum_{c \in C} (x(n,c) \cdot d(n,c)) \le T, \forall n \in N \tag{14}$$

Single assignment constraint: Each train station n is assigned to exactly one data center c.

Subject to:

$$\sum_{c \in C} x(n,c) = 1, \forall n \in N \tag{15}$$

Number of data centers constraint: There is an upper bound of K data centers that can be located in the network.

Subject to:

$$\sum_{c \in C} \delta_c \leq K \tag{16}$$

The integrity constraints for the binary variables are the following:

Active data center constraint: Data center c can only process train station n if data center c is active.

Subject to:

$$x(n,c) \leq \delta_c, \forall n \in N, \forall c \in C \tag{17}$$

Table 9 describes the allowed values that $x(n,c)$ can take depending on the value of δ_c. If the data center is not active ($\delta_c = 0$), no train station can be assigned to that data center ($x(n,c) = 0$). But if the data center is active ($\delta_c = 1$), train station n may, or may not, be assigned to data center c.

δ_c	$x(n,c)$
0	0
1	1
1	0

Table 9 Allowed values in active data center constraint of the ILP

Shortest path constraint: If train station n is being processed by data center c, the edges that are part of the shortest path from n to c must be used.

Subject to:

$$y(e,n,c) = x(n,c), \forall n \in N, \forall c \in C, \forall e \in S(n,c) \tag{18}$$

Table 10 shows the allowed values of $y(e,n,c)$ as a function of the value of $x(n,c)$. If data center c is assigned to train station n ($x(n,c) = 1$), the edges that are part of the shortest path from n to c, $S(n,c)$, have to be used ($y(e,n,c) = 1$).

$x(n,c)$	$y(e,n,c)$
0	0
1	1

Table 10 Allowed values in shortest path constraint of the ILP

4.4 Implementation

We modeled the DCPAP graph *G(N,E)* using NetworkX 2.6.2 and Python 3.8.8. The ILP model was implemented using Gurobi Optimizer 9.5.1 with the default MIPGap of 0.01% and 600s of time limit. All the simulations were performed using a laptop computer, equipped with an AMD Ryzen 7 4800H at 2.90 GHz, a Radeon graphic card, 16 GB of RAM and Windows 10 Home as operative system.

A) Link and data center costs

Concerning the link costs, they will depend on the length of the link and the traffic that passes through it. The selected link costs are based on the results from paper [44], which suggests an effective price per month per optical fiber strand in the rural environment of 0.002 €/m. We assume that a strand can transport 10 Gbps and this results in a cost of $2 \cdot 10^{-7}$ €/(Mbps·m) for the links of the core network. Then, this cost is multiplied by the length of the link to obtain the parameter p_e [EUR/Mbps]. The link cost in the rail network is half of one in the core network, $1 \cdot 10^{-7}$ €/(Mbps·m), since this infrastructure is expected to be owned by the Deutsche Bahn. As for the data center costs, they are assumed to be a fixed monthly maintenance fee between 1,000 € and 10,000 € per data center depending on the scenario, as it will be explained in Section 4.4 D).

B) Latency

This section describes the flow of the transmitted data and the computation of the end-to-end latency. It is considered, that trains are the data source, since the information from passenger services and DRO is originated in the train and sent towards the nearest macro or micro base station. We assume that this traffic is then aggregated and transported using the optical fronthaul to the nearest train station, where the BBU pools will be located. From the train stations, the data is forwarded over the optical backhaul links of the rail network or core network towards the data center, which is the destination node.

These data centers store the information of the applications that the users are trying to access through the Internet, and the critical information that rail operators need for the smooth operation of the rail services such as timetables, routes or topographic data. Only the uplink, from train to data center, is considered since the downlink end-to-end latency is assumed to be symmetric. Below, details regarding the delays at each point in the network can be found.

- **Wireless propagation delay from train to base station:** The worst case is when the train is located at the edge of the macro cell.

$$T_w = \frac{radius\ macro\ BS}{c} = \frac{4 \cdot 10^3\ m}{3 \cdot 10^8\ m/s} = 0.013\ ms$$

- **Antenna processing delay in base station** [45]:

$$T_{ant} = 0.5\ ms$$

- **Fiber propagation delay from base station to train station (fronthaul):** The distance between a train station and the macro base station that is located the farthest, which is the base station located in the middle of the link, is different for each link. Hence, the maximum link length is chosen to compute $T_{bs,ts}$ to consider the worst-case scenario.

$$T_{bs,ts} = \frac{longest\ link\ length\ between\ two\ train\ stations/2}{v} = \frac{309300/2\ m}{2 \cdot 10^8\ m/s}$$
$$= 0.77325\ ms$$

- **Train station BBU processing delay** [45]**:**

$$T_{ts} = 0.5\ ms$$

- **Fiber propagation delay from train station to data center (backhaul):** This is an input of the ILP and is computed offline by finding the shortest path between a train station and all potential data centers.

$$sp(n, c) = \frac{shortest\ path\ length}{v}, \forall\ n \in N, \forall c \in C$$

- **DCF latency:** Dispersion Compensating Fiber (DCF) accounts for the delay introduced by optical transmission systems. It is only used in long-distance networks to compensate the optical signal's dispersion. A typical long-distance network requires a DCF on approximately 20 to 25% of the overall fiber length [46].

$$T_{DCF} = 0.25 \cdot sp(n, c)$$

- **Transponder latency:** Transponders convert an optical signal to the electrical domain and back to the optical domain again (O-E-O). We consider a delay of 10 μs per transponder [46]. Two transponders are always present at the train station and at the data center.

  Additional transponder delays need to be taken into account if in the shortest path between train station and data center, there are one or more changes from the optical network of the rail operator to the core network and vice versa. In that case, an additional transponder will be needed for the O-E-O conversion. Otherwise, if the shortest path only uses optical links that are part of the same network, rail or core, it is seen as transparent and therefore there is no additional transponder delay.

$$T_{trans} = 20 + r \cdot 10\ \text{μs}, where\ r\ is\ the\ number\ of\ network\ changes$$

- **Data center processing delay:** Normal latency values in data centers are in the order of tens or hundreds of microseconds, while unexpected events, such as network congestion or packet loss, can lead to latency spikes in the order of milliseconds [47]. According to this, we assume an average delay of 0.5 ms for the worst case.

$$T_{dc} = 0.5\ ms$$

Finally, Equation (19) can be used to compute the **end-to-end latency** *d(n,c)*:

$$d(n, c) = T_w + T_{ant} + T_{bs,ts} + T_{ts} + sp(n, c) + T_{DCF} + T_{trans} + T_{dc} \ [ms] \qquad \textbf{(19)}$$

$$\boldsymbol{d(n, c)} = 0.013 + 0.5 + 0.77325 + 0.5 + sp(n, c) + 0.25 \cdot sp(n, c) + (0.02 + 0.01 \cdot r)$$
$$+ \ 0.5 = \boldsymbol{2.31 + 0.01 \cdot r + 1.25 \cdot sp(n, c)} \ [ms]$$

where r is the number of network changes in the shortest path between train station n and data center c and *sp(n,c)* is optical propagation delay following the shortest path from n to c.

C) Normalization (Bi-Objective Optimization)

The ILP problem formulation has two objectives: latency and infrastructure cost minimization. This makes it a Multi-Objective Optimization (MOO) problem. To solve it, we have used the Weighted Sum Method as seen in [48]. This method combines all the objectives into a linear combination, incorporating weights or relative importance to each of the objectives.

Nonetheless, one of the main drawbacks of this bi-objective model is that the order of magnitude for the first objective (latency in milliseconds) and the second objective (cost in EUR/month) has a great variance. This will result in the objective with a higher order of magnitude having more importance in the resolution of the MOO problem. A common approach to overcome this issue is to optimize each of the objectives individually first to find the optimal value (minimum or maximum) of each one of the objectives. Next, each objective is divided by its optimum value. Lastly, the normalized terms are summed as one objective, making this new objective dimensionless.

In our case, the single-objective models were solved to find the minimum latency, $\beta = 0$ in Equation (11), and the minimum cost, $\alpha = 0$ in the equation. After that, each minimization objective, z_d and z_c, was divided by the previously found minimum latency and cost, respectively. This means that the normalized z_d and z_c objectives will be equal to 1 when their value is the minimum, and they will have a value greater than 1 otherwise.

D) Description of the considered scenarios

Table 11 introduces the four different scenarios that have been considered for the simulations. Each case represents the variation of one of the input parameters to observe the impact on the system in terms of latency, cost, and the number of data centers K' that are needed for each case.

Scenario	Input parameters	Description
S1	$T = 10$ ms $V_c = 200$ Gbps $U_{rail} = 40$ Gbps $U_{core} = 100$ Gbps $p_c = 1{,}000$ €/month $\alpha = \beta = 1$	A low cost per data center. The variable is the maximum number of data centers that can be located in the network K. $K = (6, 7, 8, 9, 10, 11, 12, 13, 14, 15)$
S2	$T = 10$ ms $K = 10$ $V_c = 200$ Gbps $U_{rail} = 40$ Gbps $U_{core} = 100$ Gbps $p_c = 5{,}000$ €/month	A high cost per data center. The variables in the bi-objective problem formulation are the weights α and β. $(\alpha, \beta) = [(1,0), (0,1), (1,1), (1,2), (1,5), (1,10), (2,1), (3,1), (5,1), (10,1)]$
S3	$K = 10$ $V_c = 200$ Gbps $U_{rail} = 40$ Gbps $U_{core} = 100$ Gbps $p_c = 5{,}000$ €/month $\alpha = 1, \beta = 5$	A high cost per data center, the cost has a larger weight than the latency. The variable is the maximum tolerated latency T. $T = (10, 9, 8, 7, 6, 5.8, 5.6, 5.4, 5.2, 5, 4.9, 4.8)$ ms
S4	$T = 10$ ms $\alpha = 1, \beta = 5$ **S4.1** $V_c = 200$ Gbps $U_{rail} = 100$ Gbps $U_{core} = 200$ Gbps $p_c = 5{,}000$ €/month **S4.2** $V_c = 300$ Gbps $U_{rail} = 200$ Gbps $U_{core} = 300$ Gbps $p_c = 7{,}500$ €/month **S4.3** $V_c = 400$ Gbps $U_{rail} = 300$ Gbps $U_{core} = 400$ Gbps $p_c = 10{,}000$ €/month	This scenario has 3 sub-scenarios with different values for the data center and link bandwidth capacities. Note that the cost of the data center p_c increases proportionally depending on the data center processing capacity V_c. The variables are the demands of the train stations B with respect to the original bandwidth demands B_0 depicted in Figure 24. $B/B_0 = (1, 2, 3, 4, 5, 6, 7, 8, 9, 10)$

Table 11 Details of the different scenarios considered for simulation in DCPAP

4.5 Results

Results of the performed evaluations are presented here. Interpretations for the observed effects are given and the impact is discussed.

A) Scenario 1: Low cost per DC, *K* is the variable

An example of the topology that the ILP solver returns is shown in Figure 25. This is the topology for Scenario 1 with a maximum number of data centers of $K = 8$. The links of the core network are represented in white and the links of the rail network are depicted in black. Each selected data center is marked with an outer white circumference and the train stations that are assigned to that particular DC have the same color. Interestingly, we observe that clusters of train stations are formed around the data center locations. Note that the potential data center locations that have not been selected, automatically become normal train stations with a bandwidth demand that need to be assigned and routed to a data center.
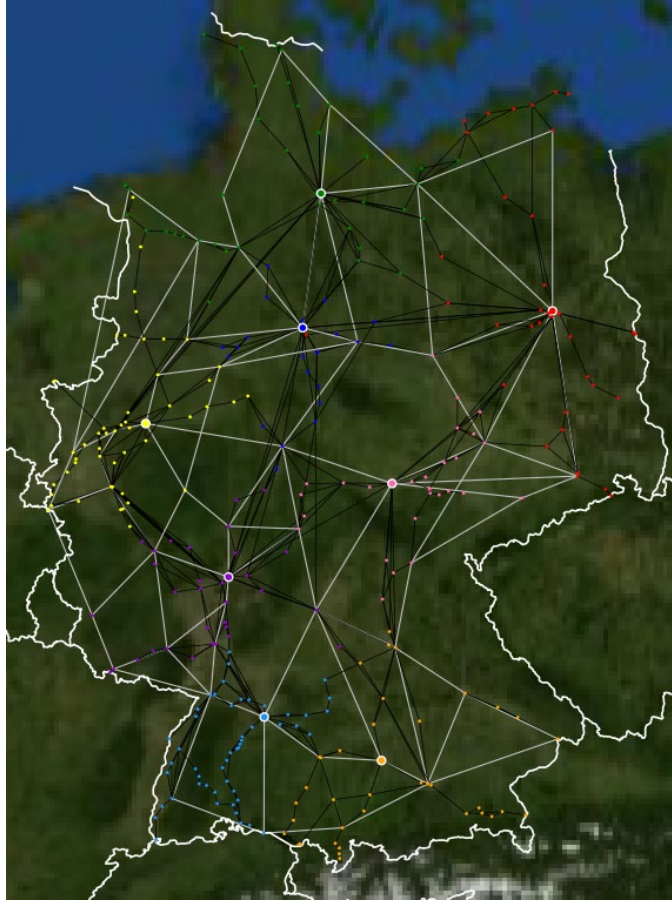
Figure 25 Example of network topology for Scenario 1 and K = 8

Table 12 shows the metrics used to analyze the performance of our model, mainly the number of DCs that have been placed in the network (K'), the latency and the cost. The cumulative latency is the value z_d in Equation (9) and the average latency is the result of dividing the cumulative latency by the number of nodes. The maximum achieved latency corresponds to the maximum value among all the latencies between a train station and its assigned DC. The total cost corresponds to z_c in Equation (10) and it has been broken down into the DC cost and the optical fiber infrastructure cost. Lastly, the computation time that Gurobi Optimizer needs to solve the ILP is shown. Similar tables for the other 3 scenarios can be found in Appendix B.

K	K'	Cumulative latency (ms)	Avg lat (ms)	Max lat (ms)	Cost (€/month)	C_{DC} (€/month)	C_{OF} (€/month)	Computation time (s)
6	6	1056.06	3.43	6.04	26,255.26	6,000	20,255.26	76.91
7	7	1026.83	3.33	4.82	23,851.25	7,000	16,851.25	59.38
8	8	995.15	3.24	4.82	23,004.24	8,000	15,004.24	38.41
9	9	983.83	3.19	4.82	23,004.41	9,000	14,004.41	39.07
10	10	970.27	3.15	4.82	23,099.11	10,000	13,099.11	42.38
11	11	961.31	3.12	4.82	23,231.96	11,000	12,231.96	41.18
12	12	953.44	3.10	4.82	23,387.70	12,000	11,387.70	40.66
13	12	953.44	3.10	4.82	23,387.70	12,000	11,387.70	40.06
14	12	953.44	3.10	4.82	23,387.70	12,000	11,387.70	39.05
15	12	953.44	3.10	4.82	23,387.70	12,000	11,387.70	37.50

Table 12 Metrics for Scenario 1 in DCPAP

Figure 26 depicts the evolution of the latency and the cost as the maximum number of data centers, that can be assigned in the network, K increases. Note that in parenthesis, next to K, the actual number of data centers K' (which is an output) that were placed in the network is shown. There is a clear trend of decreasing average latency as K increases. This is congruent with the expected results, since a larger number of DCs in the network means that a train station has more DCs nearby. Hence, the propagation delay between a train station and the closest data center will be reduced. The average latency is always below the maximum tolerated delay $T = 10$ ms required for Digital Rail Operations as described in Table 1.
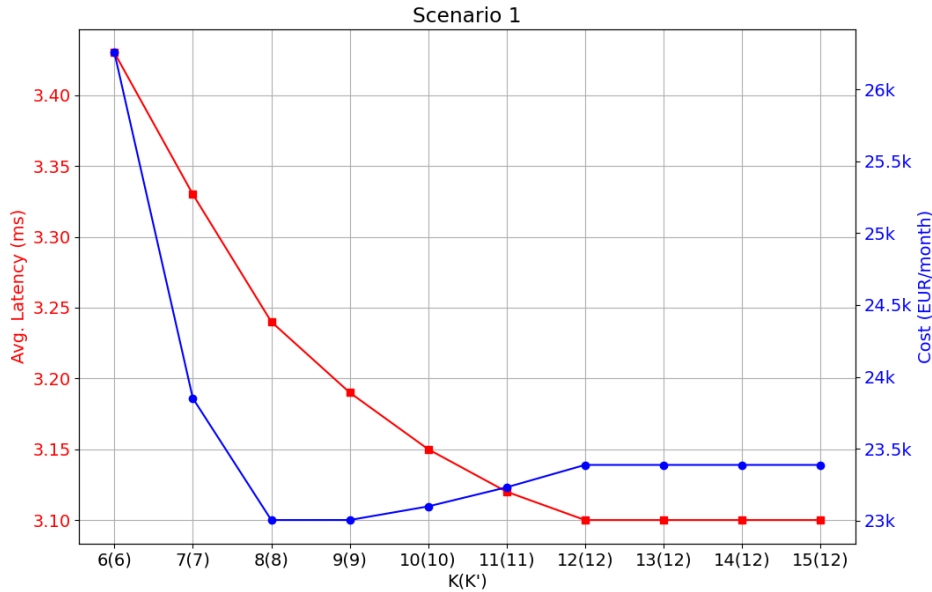
Figure 26 Average latency and cost for Scenario 1

For K between 6 and 11, the ILP solver places the maximum number of DCs in the network, i.e., $K' = K$. Interestingly, once the cost of the data centers is comparable or greater than the cost of the optical fiber, the value of K' does not increase anymore. This effect can be observed from point $K = 12$ onwards (see Table 12), where the average latency and cost are kept constant in Figure 26. A possible explanation is that in Equation (10), the total DC cost depends on the number of active DCs (output) while the cost of the optical fiber depends on the length of the links used and the traffic (input). Thus, once the cost of the data centers is comparable to the cost of the optical fiber, no more DCs are added to the network to avoid increasing the DC cost, as long as the latency and bandwidth capacity constraints are respected. This is mainly because the

bandwidth demands of the train stations are a fixed input, which cannot be changed, while the number of DCs (K') is an output that can vary to minimize the cost.

B) Scenario 2: High cost per DC, α and β are the variables

Figure 27 shows the Pareto Frontier of the DCPAP's solution space as we change the value of the weights α and β. We can observe the trade-off between latency and cost. With higher values of α, more importance is given to minimize the latency but consequently the cost of the system is higher. Whereas for higher values of β, minimizing the cost has a higher priority and the average latency increases. However, it is always below the maximum tolerated delay $T = 10$ ms, as this is a constraint in the ILP.

Another important result is that for $\beta \geq \alpha$, K' is always 6. Six is the minimum number of DCs that are needed to meet the bandwidth demands (1,087,402 Mbps) of the train stations with a DC capacity of 200 Gbps. This means that our model is able to place the minimum number of DCs, that are needed to satisfy the bandwidth demands, in order to minimize the cost when we have a high DC cost like in Scenario 2.
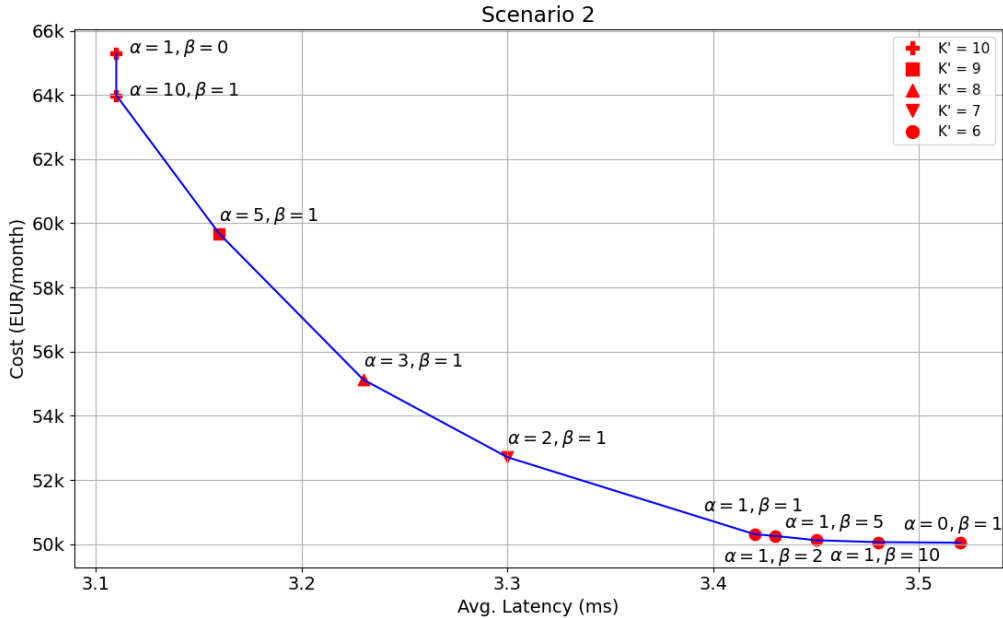
Figure 27 Pareto Frontier for Scenario 2

C) Scenario 3: High cost per DC, $\alpha < \beta$

From what we have observed in Scenarios 1 and 2, the maximum tolerated delay of $T = 10$ ms is a very relaxed constraint that can be easily fulfilled. For instance, Germany has an extension of 876 km x 640 km from north to south and from east to west, respectively. This corresponds to a maximum optical fiber propagation delay of $\Delta t = 876,000/(2 \cdot 10^8) = 4.38$ ms in the hypothetic and unrealistic case of a train station located in the most northern part of the country and a DC in the southern border.

In this third scenario, the maximum tolerated latency T has been decreased in each execution. As illustrated in Figure 28, for values of T between 4.9 and 5.8 ms, the maximum latency increases while the cost decreases (trade-off between cost and latency). For T between 6 and 10 ms the cost is kept constant and the maximum latency too, i.e., the ILP solver returns the same topology.
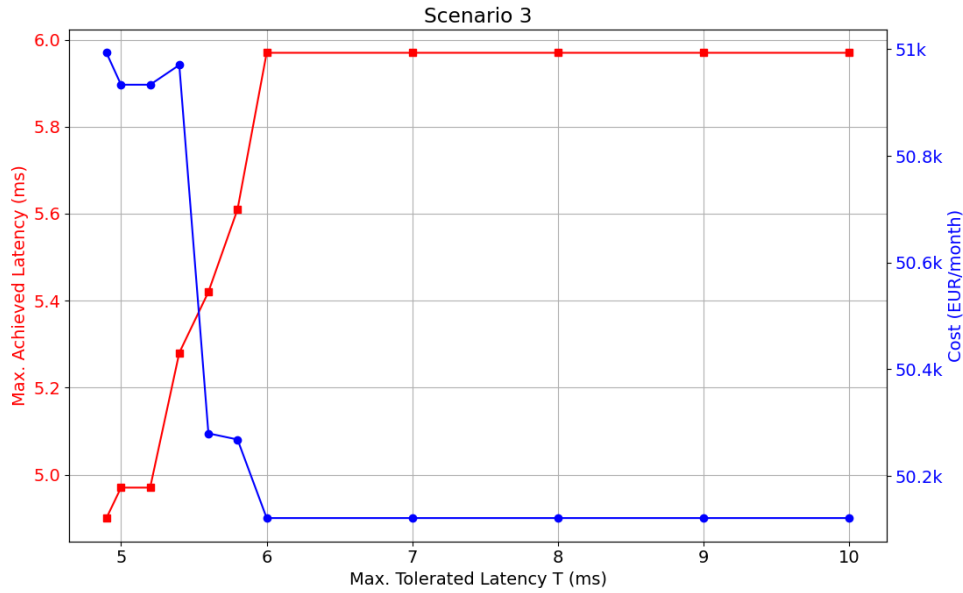
Figure 28 Maximum achieved latency and cost for Scenario 3

The most valuable finding of this experiment was that the model becomes infeasible for $T \leq 4.8$ ms. To find the reason why this happens, the minimum latency between each train station and all of the potential data centers was computed. Then, the maximum value of these minimum latencies was extracted. This maximum value corresponds to the train station that has its closest data center the farthest away, among all the train stations. We detected this happens in the Hannover Messe/Laatzen station because it only has two links that connect it to Frankfurt Hbf and Berlin-Spandau. The latter is a train station but not a potential data center location. The minimum latency was found to be 4.81 ms from Hannover Messe/Laatzen to Berlin Hbf with an intermediate stop in Berlin-Spandau.

This situation can be observed in Figure 25, where a red node (Hannover Messe/Laatzen train station) is located below the navy-blue node with a white circumference (Hannover Hbf data center). This is an anomaly since the rest of the train station nodes near the Hannover Hbf data center node are marked in blue, forming a cluster, except for that red train station node. But since there is no direct link between Hannover Messe/Laatzen and Hannover Hbf, the Hannover Messe/Laatzen train station has to be assigned to the Berlin Hbf data center, making it a red node instead of a blue one.

D) Scenario 4: 3 sub-scenarios with different DC and link bandwidth capacities

Figure 29 represents the evolution of the average latency and cost for the three sub-scenarios described in Table 11. As we can observe, the latency tends to decrease whereas the cost tends to increase, as the bandwidth demand of the train stations B increases proportionally in comparison to the original bandwidth demand B_0. This is because when the bandwidth demand increases, more data centers need to be placed in the network. Thus, reducing the average latency and increasing the cost. A more in-depth analysis between the 3 sub-scenarios with the blue, orange and green lines is presented below.

In the case of the average latency depicted in Figure 29a, it increases when the capacity of the DC increases (compare the different lines for the same B/B_0 value). This is due to the fact that for higher data center capacities (C_{DC}), the number of required data centers (K') is lower for the same bandwidth demand. Hence, the distance between a train station and its closest DC is longer. In relation to the cost depicted in Figure 29b, a similar behavior can be observed, i.e., for the same bandwidth demand, if the capacity of the DC increases, the cost also increases. This is because the monthly cost per DC increases proportionally depending on the bandwidth capacity of the DC, as explained in Table 11.

The system reaches its limit when the traffic of the train station with the highest bandwidth demand (40 Gbps in the original scenario) is greater than the data center's processing capacity. This happens at $B/B_0=5$ for the blue line, $B/B_0=8$ for the orange line and $B/B_0=10$ for the green line.
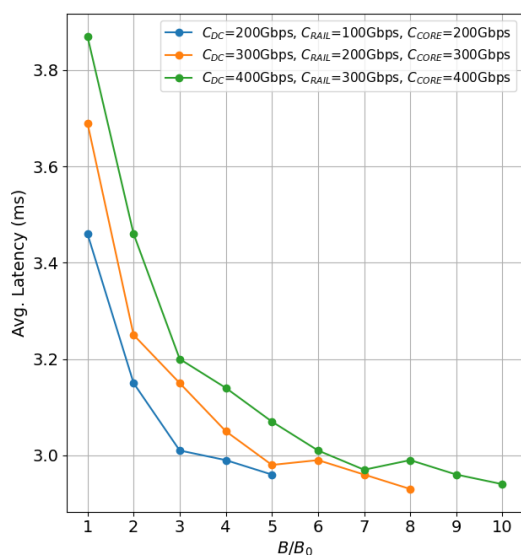
Figure 29a Average latency for Scenario 4
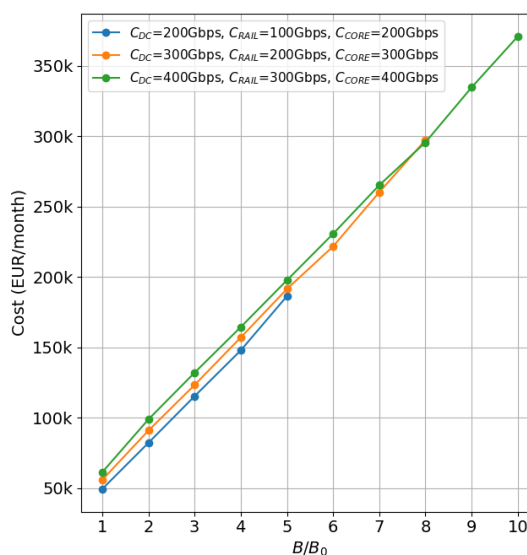
Figure 29b Cost for Scenario 4

Next, the percentage of traffic that travels through the optical network of the rail operator or the core network is depicted in Figure 30. It is clear that over 80% of all the traffic travels through the rail network in all cases, as it was expected, because the cost to use the railway operator's optical network is half of the core network's cost.

We also observe that for higher bandwidth demands of the train stations (B/B_0), the percentage of traffic in the rail network tends to increase. Note that the cost of optical fiber not only depends on the length of the link but also on the traffic in Mbps that goes through the link. Therefore, it is coherent that for higher bandwidth demands, more traffic is sent using the rail network in order to minimize the cost.
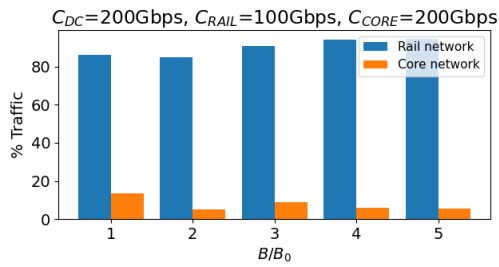
Figure 30a Percentage of traffic in the rail and core network for Scenario 4.1
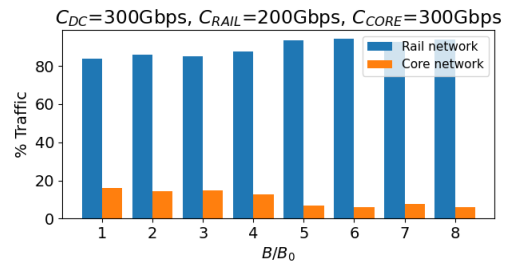
**Figure 30b** Percentage of traffic in the rail and core network for Scenario 4.2
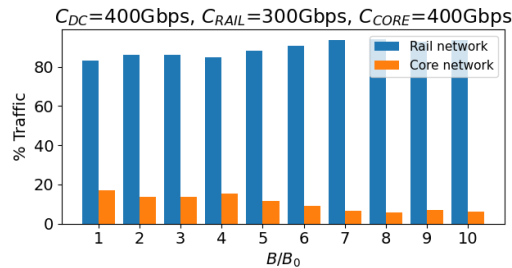
Figure 30c Percentage of traffic in the rail and core network for Scenario 4.3

## E) Most frequent data center locations and centrality measurements

The cities, where data centers are being placed more frequently, should be taken into special consideration by the network operator. Because in these locations, there is a higher likelihood that DRO and passenger connectivity applications will be placed.

Figure 31 depicts a histogram with the frequency at which a certain data center is selected by the ILP solver. The results correspond to all the simulations made for the four considered scenarios. Three levels are defined, depicted with dashed lines, to categorize the cities more frequently selected by the ILP into high, medium and low frequency.
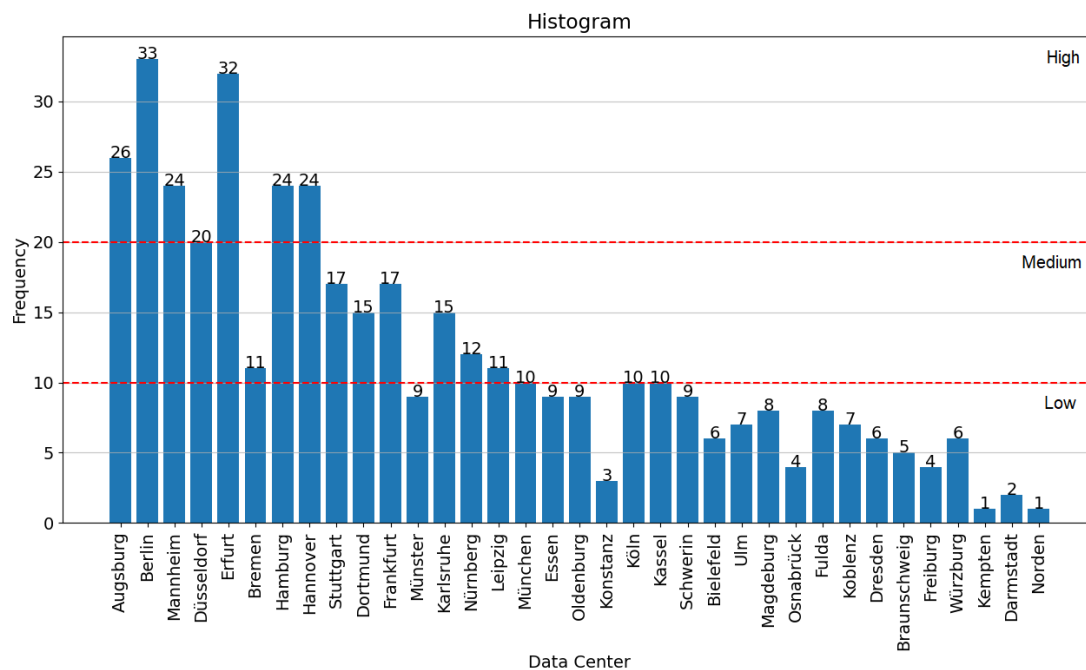
Figure 31 Histogram most frequent data center locations

Based on the previous histogram, a ranking of the data center locations with a higher probability of being used was made. This is shown in the map of Figure 32. Dark red nodes represent a high selection frequency, green is medium frequency and dark blue indicates low frequency. The data centers that have not been selected in any execution are shown in black.
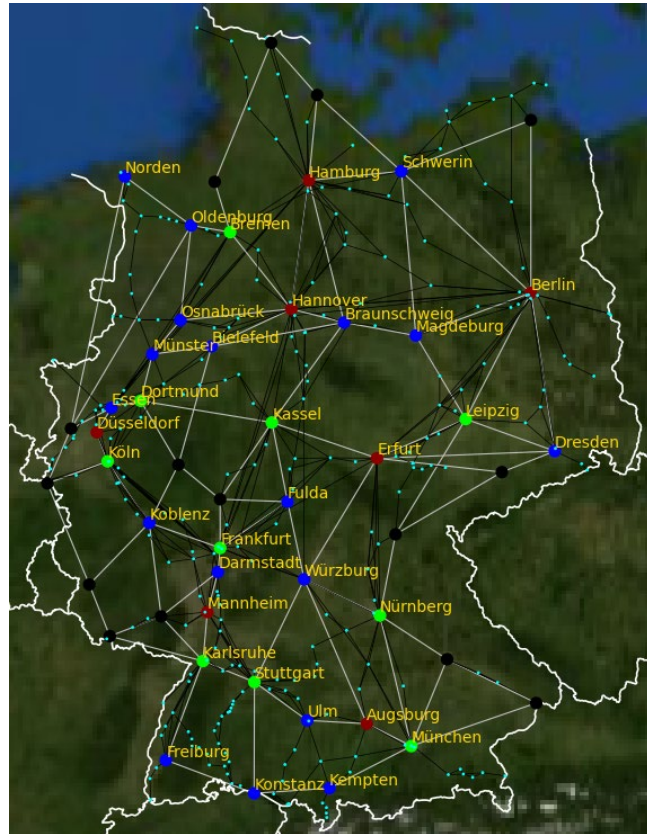
Figure 32 Data center location frequency map

Next, the data center location frequency map shown in Figure 32 is compared to the degree centrality and closeness centrality of the graph depicted in Figure 33 and Figure 34. This is done to determine whether a decision rule can be found to choose which cities should house the data centers based on the centrality measurements of the graph.
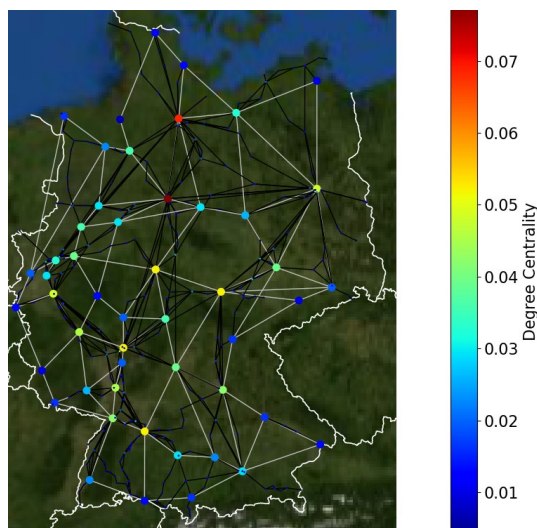
Figure 33 Degree centrality map
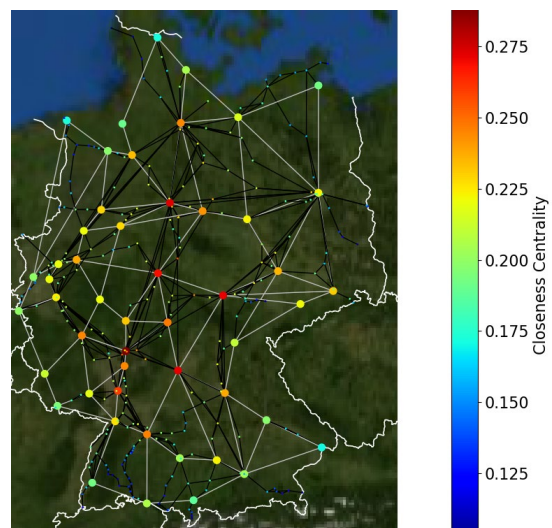
Figure 34 Closeness centrality map

The degree of a node is defined as the number of connecting edges that it has. From Figure 33, it is visible that the two nodes with the highest degree centrality (marked in red) also have a high frequency, corresponding to the cities of Hamburg and Hannover. In addition, the nodes with a low degree centrality (dark blue color) correspond to nodes with a low selection frequency or to nodes that have not been selected in any of the executions. These are mostly train stations located in cities near the border. Nevertheless, from the degree centrality map it is complicated to obtain a decision rule to classify the data centers, between high and medium frequency, since these nodes have mixed degree centrality values. The only exceptions are Hamburg and Hannover which are clearly marked in red in Figure 33 and have a high selection frequency.

The closeness centrality is the inverse of the average shortest distance between a node and all other nodes in the network. Consequently, a low closeness centrality implies a large distance of a node to the other nodes in the graph. In Figure 32, the cities of Hannover, Erfurt and Mannheim have a high selection frequency. They also have a high closeness centrality as shown in Figure 34. However, the rest of the nodes that have similar closeness centrality values (for instance the ones marked in orange) have different frequency levels.

To sum up, no general decision rules can be extracted from the degree and closeness centrality measurements to prioritize some cities over others to house data centers. Nonetheless, they might be useful to make an initial screening and rule out some potential data center locations or to assign them a low selection frequency (black and blue nodes in Figure 32) in big graphs with the goal of reducing the computation time. It is worth nothing that the centrality measurements do not take into account the maximum tolerated latency, the capacity of the DCs and the optical link capacity constraints, so the ILP formulation is still needed to make a final decision.

Chapter 5

Conclusions and Outlook

In this thesis, we planned the network for the future communications of the Deutsche Bahn's long-distance railway system in Germany. In particular, we reviewed the state of the art in order to propose a network architecture suitable for the rail environment. This network architecture is based on:

- 5G and hybrid networking (sub-6GHz and mmWave frequency bands) to meet different performance requirements of train-related and passenger-oriented applications.
- C-RAN architecture with centralized management and interference mitigation by means of CoMP.
- Two-hop model (access point − mobile relay − base station) to avoid penetration losses caused by the train's metal body.
- Optical fiber backhaul based on Ethernet to overcome the fronthaul capacity bottleneck and u-DWDM-PON to cope with massive small cell deployment.
- Core and regional data centers to run applications related to railway use cases for DRO and passenger connectivity.

We presented an approach to solve the Base Station Placement Problem (BSPP). We first used a 3GPP RMa propagation model to determine the SNR, throughput and coverage radius of the base stations by means of a link budget computation. Then, an algorithm was described to place the macro and micro base stations along the rail tracks and to obtain an approximation of the number of base stations that are required. We found that 4,252 macro base stations with an ISD of 8.3 km and 31,616 micro base stations with and ISD of 1.1 km are needed to guarantee 60 Mbps of cell edge throughput in the macro BS and 1 Gbps of cell edge throughput in the micro BS.

Similarly, we performed an analysis of the Data Center Placement and Assignment Problem (DCPAP). An ILP-based optimization model was built using NetworkX and Gurobi Optimizer with three goals: finding the required number of data centers and their location in the network, assigning one data center to each train station, and conducting the routing between the train station and its assigned data center. We demonstrated the feasibility of solving the DCPAP using an ILP formulation. Simulations in four different scenarios were performed to observe the impact of modifying different input parameters (e.g., maximum tolerated delay and maximum number of DCs) on the achieved latency and cost.

The results of the simulations showed a trade-off between the latency and the infrastructure cost. In Scenarios 1 and 2, we found that the latency is not a limiting factor since the 10 ms latency requirement for rail applications can be easily fulfilled for Germany's rail network. Consequently, we concluded that edge data centers are not

needed. We also showed that our model is able to minimize the number of DCs when we assign a high data center cost. In Scenario 3, we found that the model becomes infeasible if we want to guarantee a latency equal or smaller than 4.8 ms for the considered topology. Scenario 4 illustrated the importance of correctly dimensioning the data center and optical link bandwidth capacities since they will be a bottleneck when the bandwidth demands increase. Lastly, we generated a map indicating the frequency a data center location is selected. The cities where data centers are being placed more frequently should be taken into special consideration by the network operator.

The model proposed in this bachelor's thesis can help rail network operators to optimize network planning to meet the future requirements of DRO and passenger connectivity. Furthermore, the input parameters can be tuned to fit their specific needs.

Future work would include the dynamic assignment of DCs for moving trains and the service migration between DCs, the study of network restoration in case of failure (e.g., optic fiber link failure), and to solve the wavelength assignment sub-problem derived from the RWA problem.

List of Figures

List of Tables

Notation and Abbreviations

3GPP	3rd Generation Partnership Project
AP	Access Point
ATO	Automatic Train Operation
AWGN	Additive White Gaussian Noise
BBU	Base Band Unit
BS	Base Station
BSPP	Base Station Placement Problem
C/U-plane	Control/User-plane
CAPEX	Capital Expenditure
CN	Core Network
CO	Central Office
CoMP	Coordinated Multi-Point
CPRI	Common Public Radio Interface
CQI	Channel Quality Indicator
C-RAN	Cloud-Radio Access Network
CU	Centralized Unit
DC	Data Center
DCF	Dispersion Compensating Fiber
DCPAP	Data Center Placement and Assignment Problem
DL	Downlink
DRO	Digital Rail Operations
DU	Distributed Unit
DWDM	Dense Wavelength Division Multiplexing
eMBB	Enhanced Mobile Broadband
eNodeB	Evolved Node B
ETCS	European Train Control System
ETSI	European Telecommunications Standards Institute
EU	European Union
FDD	Frequency Division Duplexing
FRMCS	Future Railway Mobile Communication System
gNodeB	Next Generation Node B
GoA	Grade of Automation
GSM-R	Global System for Mobile Communications – Railway
HLS	Higher Layer Split
IC/ICE	InterCity/InterCity Express
ILP	Integer Linear Programming
IM	Infrastructure Manager
ISD	Inter-Site Distance
ITU	International Telecommunication Union
LOS	Line-of-Sight
LTE	Long Term Evolution
LTE-A	LTE-Advanced
MCS	Modulation and Coding Scheme
MIMO	Multiple-Input and Multiple-Output
MNO	Mobile Network Operator
MOO	Multi-Objective Optimization
NFV	Network Function Virtualization

NLOS	Non-Line-of-Sight
NR	New Radio
OPEX	Operational Expenditure
PON	Passive Optical Network
PRB	Physical Resource Block
QoS	Quality of Service
RAN	Radio Access Network
RoF	Radio-over-Fiber
RRH	Remote Radio Head
RRU	Remote Radio Unit
RU	Radio Unit
RWA	Routing and Wavelength Assignment
SDN	Software Defined Networking
SINR	Signal to Interference plus Noise Ratio
SNR	Signal to Noise Ratio
TDD	Time Division Duplexing
TR	Technical Report
u-DWDM	Ultra Dense Wavelength Division Multiplexing
UE	User Equipment
UIC	International Union of Railways
UL	Uplink
URLLC	Ultra Reliable Low Latency
UT	User Terminal
WDM	Wavelength Division Multiplexing

Bibliography

[1]   European Comission, "The European Green Deal sets out how to make Europe the first climate-neutral continent by 2050, boosting the economy, improving people's health and quality of life, caring for nature, and leaving no one behind," 2019. [Online]. Available: https://ec.europa.eu/commission/presscorner/detail/en/ip_19_6691

[2]   European Comission, "A Europe fit for the digital age. Empowering people with a new generation of technologies," 2020. [Online]. Available: https://ec.europa.eu/info/strategy/priorities-2019-2024/europe-fit-digital-age_en

[3]   A. Varasteh *et al.*, "Mobility-Aware Joint Service Placement and Routing in Space-Air-Ground Integrated Networks," in *ICC 2019 - 2019 IEEE International Conference on Communications (ICC)*, 2019, pp. 1–7. doi: 10.1109/ICC.2019.8761265.

[4]   A. Varasteh, H. S. Frutuoso, M. He, W. Kellerer, and C. Mas-Machuca, "Figo: Mobility-Aware In-Flight Service Assignment and Reconfiguration with Deep Q-Learning," in *GLOBECOM 2020 - 2020 IEEE Global Communications Conference*, 2020, pp. 1–7. doi: 10.1109/GLOBECOM42002.2020.9322493.

[5]   R. He *et al.*, "High-Speed Railway Communications: From GSM-R to LTE-R," *IEEE Vehicular Technology Magazine*, vol. 11, no. 3, pp. 49–58, 2016, doi: 10.1109/MVT.2016.2564446.

[6]   International Union of Railways (UIC), "Future Railway Mobile Communication System User Requirements Specification," 2020, [Online]. Available: https://uic.org/IMG/pdf/frmcs_user_requirements_specification-fu_7100-v5.0.0.pdf

[7]   European Union Agency for Railways (ERA), "Technical Specifications for Interoperability." https://www.era.europa.eu/activities/technical-specifications-interoperability_en

[8]   EIM and CER, "Strategic Deployment Agenda '5G Connectivity and spectrum for rail,'" Apr. 2020.

[9]   International Union of Railways (UIC), "Future Railway Mobile Communication System." https://uic.org/rail-system/frmcs/

[10]   CEPT, "ECC Decision (20)02," Nov. 2020, [Online]. Available: https://docdb.cept.org/download/1446

[11]   Ericsson and Deutsche Bahn, "Design of an FRMCS 5G E2E System for Future Rail Operation - White Paper," 2021.

[12]   Deutsche Bahn, "WLAN im ICE: So nutzen Sie das Internet im Zug." https://www.bahn.de/service/zug/wlan-im-zug

[13]   5G PPP, "D2.1 5G VICTORI Use case and requirements definition and reference architecture for vertical services," Dec. 2019, [Online]. Available: https://www.5g-victori-project.eu/

[14]   B. Ai, A. F. Molisch, M. Rupp, and Z. D. Zhong, "5G key technologies for smart railways," *Proceedings of the IEEE*, vol. 108, no. 6, pp. 856–893, Jun. 2020, doi: 10.1109/JPROC.2020.2988595.

[15]   L. Yan, X. Fang, X. Wang, and B. Ai, "AI-Enabled Sub-6-GHz and mm-Wave Hybrid Communications: Considerations for Use with Future HSR Wireless Systems," *IEEE Vehicular Technology Magazine*, vol. 15, no. 3, pp. 59–67, Sep. 2020, doi: 10.1109/MVT.2020.2969528.

[16] GSMA, "Mobile Backhaul: An Overview - Future Networks." https://www.gsma.com/futurenetworks/wiki/mobile-backhaul-an-overview/

[17] D. Gesbert, S. Hanly, H. Huang, S. Shamai Shitz, O. Simeone, and W. Yu, "Multi-Cell MIMO Cooperative Networks: A New Look at Interference," *IEEE Journal on Selected Areas in Communications*, vol. 28, no. 9, pp. 1380–1408, 2010, doi: 10.1109/JSAC.2010.101202.

[18] CPRI Specification V6.1, "Common Public Radio Interface (CPRI); Interface Specification," 2014, [Online]. Available: http://www.cpri.infohttp://www.cpri.info/spec.html

[19] T. Pfeiffer, "Next generation mobile fronthaul architectures," in *2015 Optical Fiber Communications Conference and Exhibition (OFC)*, 2015, pp. 1–3. doi: 10.1364/OFC.2015.M2J.7.

[20] K. Tanaka and A. Agata, "Next-generation optical access networks for C-RAN," in *2015 Optical Fiber Communications Conference and Exhibition (OFC)*, 2015, pp. 1–3. doi: 10.1364/OFC.2015.Tu2E.1.

[21] C. Liu, L. Zhang, M. Zhu, J. Wang, L. Cheng, and G.-K. Chang, "A Novel Multi-Service Small-Cell Cloud Radio Access Network for Mobile Backhaul and Computing Based on Radio-Over-Fiber Technologies," *Journal of Lightwave Technology*, vol. 31, no. 17, pp. 2869–2875, 2013, doi: 10.1109/JLT.2013.2274193.

[22] S. Sarmiento, J. A. Altabas, S. Spadaro, and J. A. Lazaro, "Experimental Assessment of 10 Gbps 5G Multicarrier Waveforms for High-Layer Split U-DWDM-PON-Based Fronthaul," *Journal of Lightwave Technology*, vol. 37, no. 10, pp. 2344–2351, 2019, doi: 10.1109/JLT.2019.2904114.

[23] H. Kim, "RoF-based Optical Fronthaul Technology for 5G and Beyond," in *2018 Optical Fiber Communications Conference and Exposition (OFC)*, 2018, pp. 1–3.

[24] TelecomHall Forum, "What is Fronthaul, Midhaul and Backhaul in 5G?" https://www.telecomhall.net/t/what-is-fronthaul-midhaul-and-backhaul-in-5g/16985

[25] J. K. Chaudhary, "Analysis of Bandwidth and Latency Constraints on a Packetized Cloud Radio Access Network Fronthaul," PhD Dissertation, Technische Universität Dresden, 2020.

[26] International Telecommunication Union, "10-Gigabit-capable symmetric passive optical network (XGS-PON)," *ITU-T G.9807 Series of Recommendations*, 2016, [Online]. Available: https://www.itu.int/rec/T-REC-G.9807.1-201606-I/en

[27] H. Rohde *et al.*, "Coherent Ultra Dense WDM Technology for Next Generation Optical Metro and Access Networks," *Journal of Lightwave Technology*, vol. 32, no. 10, pp. 2041–2052, 2014, doi: 10.1109/JLT.2014.2316369.

[28] J. Kani, J. Terada, K.-I. Suzuki, and A. Otaka, "Solutions for Future Mobile Fronthaul and Access-Network Convergence," *Journal of Lightwave Technology*, vol. 35, no. 3, pp. 527–534, 2017, doi: 10.1109/JLT.2016.2608389.

[29] P. Chanclou, L. A. Neto, K. Grzybowski, Z. Tayq, F. Saliou, and N. Genay, "Mobile fronthaul architecture and technologies: A RAN equipment assessment," in *2017 Optical Fiber Communications Conference and Exhibition (OFC)*, 2017, pp. 1–3.

[30] Nokia and Deutsche Bahn, "Highly resilient FRMCS/5G design for future rail operation - White Paper," 2021.

[31] ITU-T G Suppl. 66, "5G wireless fronthaul requirements in a passive optical network context," 2019.

[32] ETSI, "TR 103 554-2 - Rail Telecommunications (RT); Next Generation Communication System; Radio performance simulations and evaluations in rail environment; Part 2: New Radio (NR)," Feb. 2021.

[33] Techplayon, "5G Network RF Planning - Link Budget Basics." https://www.techplayon.com/5g-network-rf-planning-link-budget-basics/

[34] ETSI, "TR 138 901 - V16.1.0 - 5G; Study on channel model for frequencies from 0.5 to 100 GHz (3GPP TR 38.901 version 16.1.0 Release 16)," 2020.

[35] "GTFS für Deutschland." https://gtfs.de/

[36] ETSI, "TR 138 913 - 5G; Study on scenarios and requirements for next generation access technologies (3GPP TR 38.913 version 17.0.0 Release 17)," May 2022.

[37] Techplayon, "5G NR SINR Measurement and Its Mapping." https://www.techplayon.com/5g-nr-sinr-measurement-and-its-mapping/

[38] ETSI, "TS 138 133 - V15.3.0 - 5G; NR; Requirements for support of radio resource management (3GPP TS 38.133 version 15.3.0 Release 15)," 2018.

[39] ITU-R, "Calculation of free-space attenuation. P Series. Radiowave propagation".

[40] "What is a Data Center?," *Palo Alto Networks*. https://www.paloaltonetworks.com/cyberpedia/what-is-a-data-center

[41] I. Chlamtac, A. Ganz, and G. Karmi, "Lightpath communications: an approach to high bandwidth optical WAN's," *IEEE Transactions on Communications*, vol. 40, no. 7, pp. 1171–1182, 1992, doi: 10.1109/26.153361.

[42] SDNlib, "Problem germany50--D-B-L-N-C-A-N-N." http://sndlib.zib.de/home.action?show=/problem.details.action%3FproblemNa me%3Dgermany50--D-B-L-N-C-A-N-N%26frameset

[43] M. Klinkowski, K. Walkowiak, and R. Goścień, "Optimization algorithms for data center location problem in Elastic Optical Networks," in *2013 15th International Conference on Transparent Optical Networks (ICTON)*, 2013, pp. 1–5. doi: 10.1109/ICTON.2013.6602815.

[44] CTC Technology & Energy, "Dark Fiber Lease Considerations," 2012.

[45] R. Bonk, T. Pfeiffer, and B. Powell, "Latency Challenges for 25/50/100G EPON," 2017.

[46] Infinera, "Low Latency-How Low Can You Go? Background and Drivers," 2020.

[47] D. A. Popescu, "Latency-driven performance in data centres," *University of Cambridge Computer Laboratory*, 2019.

[48] E. Sakic, N. Deric, E. Goshi, and W. Kellerer, "P4BFT: Hardware-Accelerated Byzantine-Resilient Network Control Plane," in *2019 IEEE Global Communications Conference (GLOBECOM)*, 2019, pp. 1–7. doi: 10.1109/GLOBECOM38437.2019.9013772.

Appendix A

SNR and throughput considering the effect of slow fading

The received power at a certain distance taking into account the slow fading, also known as the local average received power (P_r), can be expressed as:

$$P_r = \frac{P_R}{A_f} = \frac{P_T G_T G_R}{L \, A_f}$$

where P_R is the nominal received power and A_f is the slow fading (shadowing).

P_r follows a log-normal distribution:

$$f_{P_r}(P_r) = \frac{1}{\sqrt{2\pi}\sigma} e^{-\frac{(P_r - P_R)}{2\sigma^2}}$$

where σ is the typical deviation of the slow fading, which depends on the environment, and the powers are expressed in dBm.

The probability that the average received power is above a threshold can be computed as:

$$p = \text{Prob}(P_r \geq P_s) = \frac{1}{\sqrt{2\pi}\,\sigma} \int_{P_s}^{\infty} e^{-\frac{(P_r - P_R)}{2\sigma^2}} dP_r = \frac{1}{2} + \frac{1}{2} \cdot \text{erf}(\frac{P_R - P_s}{\sqrt{2}\,\sigma})$$

Considering the worst-case scenario, we can calculate the fade margin as follows assuming a 99% probability and a typical deviation of 4 dB given in the RMa model in Table 3.

$$MF \ (dB) = P_R(dBm) - P_s(dBm) = \sqrt{2}\,\sigma\,erf^{-1}(2p - 1) = \sqrt{2} \cdot 4 \cdot erf^{-1}(2 \cdot 0.99 - 1)$$
$$= \sqrt{2} \cdot 4 \cdot 1.65 = 9.33 \ dB$$

And finally, the minimum average SNR is:

$$SNR_{\min}(dB) = SNR_{nom}(dB) - MF \ (dB)$$

where SNR_{nom} is the nominal SNR that has been used in Section 3.3.

In order to keep a similar coverage radius for the same cell edge throughput, Multiple-Input-Multiple-Output (MIMO) technology can be used. If MIMO is used, the channel capacity formula is modified as follows:

$$C = Z \cdot B \cdot \log_2(1 + SNR), \qquad Z = \min(N_{TX}, N_{RX})$$

where Z is the minimum between the number of antennas in the transmitter and the receiver.

The graphs depicting the *SNR*_{*min*} and the uplink bit rate when considering the effect of the slow fading at the macro base station are shown below. As we can observe in Figure 36, the coverage radius for the same cell edge throughput of 60 Mbps is smaller than in the calculations using the nominal SNR without considering the slow fading. However, with the use of MIMO we can achieve a larger coverage radius as seen in Figure 37.
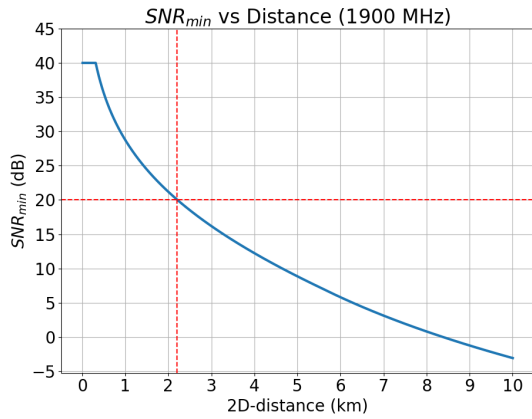
Figure 35 Minimum average SNR macro BS slow fading
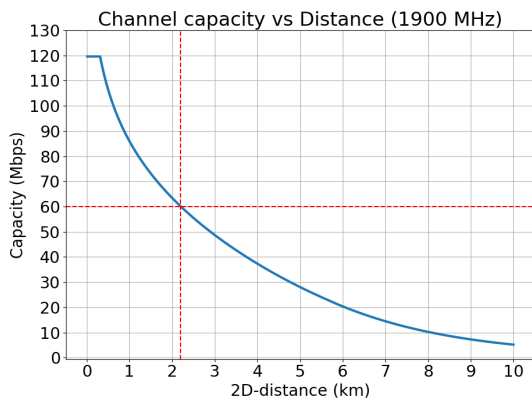
Figure 36 UL data rate macro BS slow fading
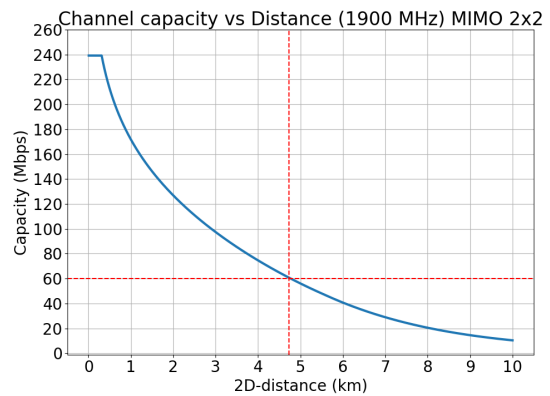
Figure 37 UL data rate macro BS slow fading MIMO 2x2

60

The following graphs show the *SNRmin* and the downlink bit rate when considering the effect of the slow fading at the micro base station. In this case, MIMO 4x4 is needed to keep the same coverage radius as in the nominal SNR scenario.
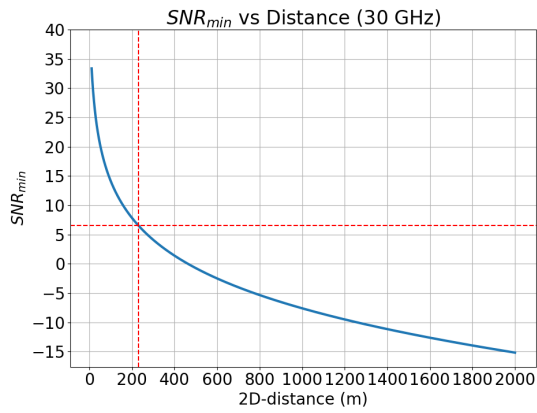
Figure 38 Minimum average SNR micro BS slow fading
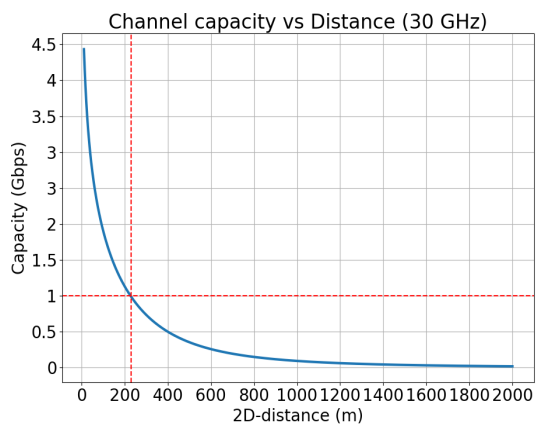
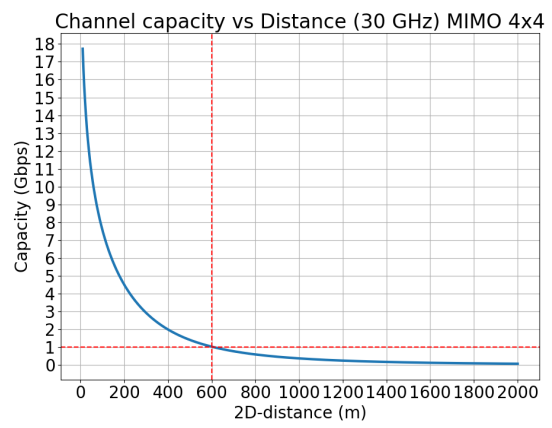**Figure 39** DL data rate micro BS slow fading

Figure 40 DL data rate micro BS slow fading MIMO 4x4

Appendix B

Simulation results in DCPAP

In this appendix, the tables with the performance metrics of the three other scenarios considered in the DCPAP simulations of Section 4.5 are shown.

Scenario 2:

α	β	K'	Cumulative latency(ms)	Avg lat(ms)	Max lat(ms)	Cost (€/month)	C_{DC} (€/month)	C_{OF} (€/month)	Comp. time(s)
1	0	10	956.72	3.11	4.82	65,282.95	50,000	15,282.9	12.61
0	1	6	1084.21	3.52	6.30	50,044.75	30,000	20,044.7	168.41
1	1	6	1054.82	3.42	5.42	50,310.17	30,000	20,310.17	277.97
1	2	6	1056.06	3.43	6.78	50,255.26	30,000	20,255.26	303.54
1	5	6	1063.30	3.45	6.22	50,121.14	30,000	20,121.14	300.27
1	10	6	1073.08	3.48	6.22	50,061.31	30,000	20,061.31	672.32
2	1	7	1015.76	3.30	4.82	52,709.16	35,000	17,709.16	273.9
3	1	8	993.61	3.23	4.82	55,127.28	40,000	15,127.28	309.28
5	1	9	972.51	3.16	4.82	59,676.72	45,000	14,676.72	281.26
10	1	10	958.06	3.11	4.82	63,987.99	50,000	13,987.99	278.29

Table 13 Metrics for Scenario 2 in DCPAP

Scenario 3:

T (ms)	K'	Cumulative latency (ms)	Avg lat(ms)	Max lat(ms)	Cost (€/month)	C_{DC} (€/month)	C_{OF} (€/month)	Comp. time(s)
10	6	1063.30	3.45	5.97	50,121.14	30,000	20,121.14	300.27
9	6	1063.30	3.45	5.97	50,121.14	30,000	20,121.14	363.51
8	6	1063.30	3.45	5.97	50,121.14	30,000	20,121.14	217.50
7	6	1063.30	3.45	5.97	50,121.14	30,000	20,121.14	363.50
6	6	1063.30	3.45	5.97	50,121.14	30,000	20,121.14	229.67
5.8	6	1056.13	3.43	5.61	50,268.37	30,000	20,268.37	58.54
5.6	6	1055.54	3.43	5.42	50,279.84	30,000	20,279.84	51.41
5.4	6	1052.30	3.42	5.28	50,970.25	30,000	20,970.25	126.17
5.2	6	1056.48	3.43	4.97	50,933.34	30,000	20,933.34	50.14
5	6	1056.48	3.43	4.97	50,933.34	30,000	20,933.34	84.97
4.9	6	1053.07	3.4	4.90	50,993.15	30,000	20,993.15	40.17
4.8	Infeasible							

Table 14 Metrics for Scenario 3 in DCPAP

Scenario 4.1:

B	K'	Cum lat (ms)	Avg lat (ms)	Max lat (ms)	Cost (€/month)	C_{DC} (€/month)	C_{OF} (€/month)	Comp. time (s)
$1B_0$	6	1065.66	3.46	5.26	49,429.95	30,000	19,429.95	91.90
$2B_0$	11	968.80	3.15	5.50	82,199.40	55,000	27,199.40	939.88
$3B_0$	17	925.91	3.01	4.88	115,325.67	85,000	30,325.67	311.96
$4B_0$	22	922.39	2.99	4.88	147,865.74	110,000	37,865.74	261.74
$5B_0$	28	910.34	2.96	4.88	186,373.64	140,000	46,373.64	497.41

B	K'	Total traffic train link (Gbps)	% Traffic train link	Total traffic core link (Gbps)	% Traffic core link
B_0	6	1743.415	86.28%	277.200	13.72%
$2B_0$	11	2837.030	85.05%	498.498	4.95%
$3B_0$	17	3982.95	90.89%	399.03	9.11%
$4B_0$	22	5178.604	94.03%	328.972	5.97%
$5B_0$	28	6206.65	94.4%	368.075	5.6%

Table 15 Metrics for Scenario 4.1 in DCPAP

Scenario 4.2:

B	K'	Cum lat (ms)	Avg lat (ms)	Max lat (ms)	Cost (€/month)	C_{DC} (€/month)	C_{OF} (€/month)	Comp. time (s)
$1B_0$	4	1135.56	3.69	5.81	55,911.31	30,000	25,911.31	55.48
$2B_0$	8	1001.08	3.25	4.82	90,912.56	60,000	30,912.56	50.08
$3B_0$	11	968.80	3.15	5.50	123,299.10	82,500	40,799.10	229.08
$4B_0$	15	939.28	3.05	5.49	157,059.66	112,500	44,559.66	197.56
$5B_0$	19	919.20	2.98	4.88	191,479.92	142,500	48,979.92	554.79
$6B_0$	22	922.21	2.99	4.88	221,694.46	165,000	56,694.46	195.02
$7B_0$	26	911.11	2.96	5.35	260,174.53	195000	65,174.53	577.61
$8B_0$	30	902.02	2.93	4.88	297,191.32	225,000	72,191.32	567.72

B	K'	Total traffic train link (Gbps)	% Traffic train link	Total traffic core link (Gbps)	% Traffic core link
$1B_0$	5	2111.434	83.8%	408.168	16.2%
$2B_0$	8	3038.056	85.83%	501.594	14.17%
$3B_0$	11	4255.545	85.05%	747.747	14.95%
$4B_0$	15	5294.392	87.51%	755.404	12.49%
$5B_0$	19	6569.695	93.33%	469.605	6.67%
$6B_0$	22	7761.816	94.2%	478.218	5.8%
$7B_0$	26	8661.107	92.49%	703.619	7.51%
$8B_0$	30	10117.624	93.97%	649.8	6.03%

Table 16 Metrics for Scenario 4.2 in DCPAP

Scenario 4.3:

B	K'	Cum lat (ms)	Avg lat (ms)	Max lat (ms)	Cost (€/month)	C_{DC} (€/month)	C_{OF} (€/month)	Comp. time (s)
$1B_0$	3	1192.53	3.87	7.17	61,318.52	30,000	31,318.52	63.27
$2B_0$	6	1065.66	3.46	5.26	98,859.89	60,000	38,859.89	110.98
$3B_0$	9	984.21	3.20	4.82	132,050.74	90,000	42,050.74	42.13
$4B_0$	11	968.15	3.14	5.50	164,423.83	110,000	54,423.83	182.99
$5B_0$	14	945.96	3.07	5.03	197,675.66	140,000	57,675.66	356.83
$6B_0$	17	925.91	3.01	4.88	230,651.34	170,000	60,651.34	130.55
$7B_0$	20	913.84	2.97	4.88	265,159.70	200,000	65,159.70	242.77
$8B_0$	22	922.08	2.99	5.58	295,600.07	220,000	75,600.07	283.17
$9B_0$	25	911.03	2.96	5.35	334,609.90	250,000	84,609.90	794.45
$10B_0$	28	906.99	2.94	5.03	370,805.33	280,000	90,805.33	461.56

B	K'	Total traffic train link (Gbps)	% Traffic train link	Total traffic core link (Gbps)	% Traffic core link
$1B_0$	4	2538.356	83.02%	519.344	16.98%
$2B_0$	7	3486.83	86.28%	554.4	13.72%
$3B_0$	9	4473.381	86.21%	715.827	13.79%
$4B_0$	11	5649.7	84.79%	1013.236	15.21%
$5B_0$	14	6729.65	88.25%	896.035	11.75%
$6B_0$	17	7965.9	90.89%	798.06	9.11%
$7B_0$	21	9030.553	93.49%	629.013	6.51%
$8B_0$	22	10381.584	94.21%	637.624	5.79%
$9B_0$	25	11254.383	92.87%	863.541	7.13%
$10B_0$	28	13266.43	93.79%	878.23	6.21%

Table 17 Metrics for Scenario 4.3 in DCPAP